Available online at www.sciencedirect.com
SCIENCE DIRECT®
Journal of Sound and Vibration 265 (2003) 123–154
JOURNAL OF SOUND AND VIBRATION
www.elsevier.com/locate/jsvi

The effects of large vibration amplitudes on the axisymmetric mode shapes and natural frequencies of clamped thin isotropic circular plates. Part I: iterative and explicit analytical solution for non-linear transverse vibrations

M. Haterbouch[a], R. Benamar[b,*]

[a] *Faculté des Sciences et Techniques, Département de Physique, Laboratoire de Mécanique et Calcul Scientifique, LMCS, BP. 509 Boutalamine, Errachidia, Morocco*

[b] *Ecole Mohammadia d'Ingénieurs, Département des E.G.T, Laboratoire d'Etudes et de Recherches en Simulation, Instrumentation et Mesures, LERSIM, BP. 765 Agdal, Rabat, Morocco*

Received 12 March 2002; accepted 15 July 2002

Abstract

The effects of large vibration amplitudes on the first two axisymmetric mode shapes of clamped thin isotropic circular plates are examined. The theoretical model based on Hamilton's principle and spectral analysis developed previously by Benamar et al. for clamped–clamped beams and fully clamped rectangular plates is adapted to the case of circular plates using a basis of Bessel's functions. The model effectively reduces the large-amplitude free vibration problem to the solution of a set of non-linear algebraic equations. Numerical results are given for the first and second axisymmetric non-linear mode shapes for a wide range of vibration amplitudes. For each value of the vibration amplitude considered, the corresponding contributions of the basic functions defining the non-linear transverse displacement function and the associated non-linear frequency are given. The non-linear frequencies associated to the fundamental non-linear mode shape predicted by the present model were compared with numerical results from the available published literature and a good agreement was found. The non-linear mode shapes exhibit higher bending stresses near to the clamped edge at large deflections, compared with those predicted by linear theory. In order to obtain explicit analytical solutions for the first two non-linear axisymmetric mode shapes of clamped circular plates, which are expected to be very useful in engineering applications and in further analytical developments, the improved version of the semi-analytical model developed by El Kadiri et al. for beams and rectangular plates, has been adapted to the case of clamped circular plates, leading to explicit expressions for the higher basic function contributions, which are shown to be in a good

*Corresponding author.
E-mail address: rbenamar@emi.ac.ma (R. Benamar).

0022-460X/03/$ - see front matter
doi:10.1016/S0022-460X(02)01443-8

agreement with the iterative solutions, for maximum non-dimensional vibration amplitude values of 0.5 and 0.44 for the first and second axisymmetric non-linear mode shapes, respectively.

1. Introduction

Thin-plate-structures are commonly used in many engineering applications, especially in the aeronautic and aerospace fields. Such structures are often subjected to severe dynamic loading conditions resulting in large vibration amplitudes. In such situations, it is not sufficient to use the classical linear theory to analyze their large vibration amplitudes behaviour. The geometric non-linearity has to be taken into account for proper design. The most widely used non-linear equations for thin plates are those originally presented by Von Kármán in the static case. Their dynamic analogue were derived by Herrmann in Cartesian co-ordinates [1]. These governing equations are either expressed in terms of the transverse and in-plane displacements, or alternatively in terms of the transverse displacement and the Airy stress function when the in-plane inertia is neglected. Due to the complexity of the governing coupled non-linear partial differential equations involved in the study of large vibration amplitude problems of thin plate-structures, no exact solution is yet known. Hence, each problem has received a special treatment involving some particular approximations. In most of the studies carried out on non-linear axisymmetric vibrations of circular plates, the common approach has been to use an assumed space or time function, it being supposed that the space and time functions can be separated. In the assumed space mode method, a spatial function which satisfies the related boundary conditions is assumed and Galerkin's method is used to eliminate the space variable from the governing equation. The problem is then reduced, in the case of the single-mode approach, to the well-known Duffing equation in time, which may be solved in terms of elliptic functions or using other methods, such as the harmonic balance method or the perturbation method. Yamaki used this technique to obtain an approximate solution based on Von Kármán equations with a single-term expansion [2]. He considered both clamped and simply supported isotropic circular plates, with stress-free and immovable boundaries. By assuming the same one-term expansion, Kung and Pao studied circular plates experimentally and analytically and found close agreement [3]. Sathyamoorthy [4] investigated the non-linear flexural vibrations of moderately thick circular plates with clamped immovable edges and found exact agreement with the results of Ref. [2] in the particular case of thin plates. Nowinski [5] investigated the large-amplitude transverse vibrations of elastic circular plates built in at the boundary by using von Kármán's dynamic equations in combination with an orthogonalization procedure in order to eliminate the space variable. He derived an approximate solution, in the time variable, in terms of elliptic functions by considering only a one-term expansion of the transverse displacement. In the assumed time function method, a simple harmonic function in time is assumed and is then eliminated from the equation of motion using Kantorovich averaging procedure. The resulting non-linear spatial boundary-value problem is solved numerically. This technique has been used with Von Kármán equations by Huang and Sandman [6], and Huang and Al-Khattat [7], to investigate non-linear free and forced vibrations of clamped circular plates, and circular plates with various boundary conditions, respectively. Some other studies [8,9] were based on a simplified non-linear differential equation, obtained by

using Berger's assumption [10], and solved by a modified Galerkin method, and a Ritz–Galerkin method, respectively. Also, a perturbation method was used to study the non-linear axisymmetric vibrations of a clamped circular plate in which the coupled non-linear Von Kármán equations as well as the simplified single non-linear plate equation obtained from Berger's hypothesis were solved [11]. Another study concerned with the effect of internal resonances on the non-linear symmetric response of clamped circular plates has been carried out in Ref. [12] by the method of multiple scales and by using the dynamic analogue of the Von Kármán equations. The two latter methods are based on perturbation procedures, and consequently, are limited to the first effects of finite displacements. Reddy and Huang [13] studied the large-amplitude free vibrations of thick, orthotropic annular plates of varying thickness by using the finite element method and a shear deformable theory. Rao et al. [14] investigated the non-linear free vibrations occurring at large vibration amplitudes of beams and orthotropic circular plates by employing the finite element method, in which a linearizing function was introduced. The formulations used in Refs. [13,14] were based on the assumption of zero in-plane radial displacement. Decha-Umphai and Mei [15], presented a finite element method to investigate non-linear forced vibrations of circular plates with various out-of-plane and in-plane boundary conditions. The in-plane deformation and in-plane inertia have been taken into account in the formulation and a linearizing function was used in the expression of the strain energy. It is to be noted here that the assumed space single-mode approach was adopted as a tool for the investigation of the effects of the geometric non-linearity on the natural frequencies and the forced vibration response [16], but it is inadequate for the estimation of the non-linear stresses as stated in Refs. [17,18]. As determination of these stresses is of great interest in engineering applications, multimode approaches are needed to obtain reliable and accurate results concerning not only the natural frequencies and the non-linear forced response [19], but also to obtain accurate stress estimates. Some investigations on the effects of higher modes, i.e., multimode analysis, on the fundamental non-linear frequencies of circular plates are reported in Refs. [20,21], in which Galerkin's method was used. On the other hand, most of the published results concerning the analysis of geometrically non-linear free vibrations of circular plates are concerned with the fundamental mode only. Experimental studies have shown that the higher modes contribute significantly to the non-linear response of beams and plates [22–24]. Therefore, the study of the higher mode contributions is indispensable in order to have a better understanding of the geometrically non-linear dynamic behaviour of plates. A theoretical model, based on Hamilton's principle and spectral analysis has been developed to analyze the dependence of the mode shapes and their corresponding frequencies on the amplitude of vibration for thin straight structures [22]. The model was applied successfully to geometrically non-linear free and forced vibrations of various structures such as simply supported and clamped–clamped beams, homogeneous and composite rectangular plates, and shells [16–18,25–32]. The main feature of the approach mentioned above is that it makes the geometrically non-linear effects appear not only via the amplitude–frequency dependence, which was the main purpose of most of the previous studies on non-linear vibrations, but also via the dependence of the structure deflection shapes on the amplitude of vibration. This allows quantitative estimate of non-linear stresses to be obtained in sensible regions of the structure, which may be of crucial importance in the fatigue life prediction of structures working in a severe environment. In the present work, axisymmetric free large vibration amplitudes of clamped immovable thin isotropic circular plates are investigated by using and adapting the model mentioned above. By assuming harmonic

motion and expanding the transverse displacement in the form of finite series of basic functions, namely the linear free vibration modes of the clamped circular plate, obtained in terms of Bessel's functions, the discretized expressions for the total strain energy and kinetic energy have been derived. In these expressions, in addition to the classical mass and rigidity tensors, a fourth order tensor appears due to the non-linearity. The application of Hamilton's principle reduced the large-amplitude free vibration problem to a set of non-linear algebraic equations, which have been solved numerically in each case, leading to the first and second non-linear axisymmetric mode shapes of clamped circular plates. The relationships between the non-linear to linear frequency ratio, between mode shapes and non-dimensional maximum amplitude for the first two mode shapes of circular plates are discussed showing a hardening type non-linearity and the amplitude dependence of the mode shapes. Also, the influence of the non-dimensional maximum amplitude on the associated bending stress distributions is given, showing a higher rate of increase of stresses with the amplitude of vibration, compared with that predicted by linear theory.

In a recent series of papers [33–35], a practical simple "multimode theory", based on the linearization of the non-linear algebraic equations, written on the modal basis, in the neighbourhood of each resonance, has been developed for beams and fully clamped and simply supported rectangular plates. Simple explicit formulae, ready and easy to use for analytical or engineering purposes, have been derived, which allowed, via the so-called first formulation, direct calculation of the basic function contributions to the first three non-linear mode shapes of clamped–clamped beams, the first non-linear mode shape of clamped, simply supported beams, and the first two non-linear mode shapes of fully clamped rectangular plates. The purpose and the interest of this approach have been extensively discussed in the above references. The same approach is extended here to clamped circular plates in order to allow direct calculation of the first two axisymmetric non-linear mode shapes, with their associated non-linear frequencies and bending stress patterns. The results given in terms of explicit analytical solutions are discussed and compared to those obtained by the iterative solution of the corresponding set of non-linear algebraic equations, to determine accurately the limit of validity of the new approach.

2. General formulation

2.1. Problem definition

Consider a circular plate of thin uniform thickness h and radius a that is clamped along its edge. The co-ordinate system is chosen such that the middle plane of the plate coincides with the (r,θ) plane, the origin of the co-ordinate system being at the centre of the plate with the z-axis downward, as shown in Fig. 1. The plate is made of an elastic, homogeneous isotropic material. In the case of axisymmetric vibrations of the circular plate, the displacements are given by [36]

$$u_r(r,z,t) = U(r,t) - z\frac{\partial W(r,t)}{\partial r}, \quad u_\theta(r,t) = 0, \quad u_z(r,t) = W(r,t), \tag{1}$$

where U and W are the in-plane and out-of-plane displacements of the middle plane point $(r,\theta,0)$, respectively, and u_r, u_θ and u_z are the displacements along r, θ and z directions, respectively.

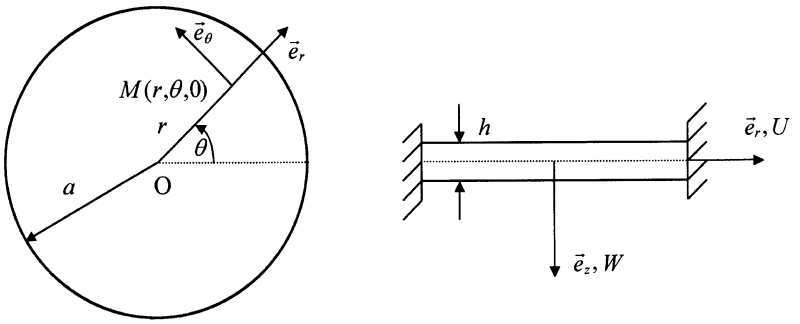

Fig. 1. Clamped circular plate notation.

The non-vanishing components of the strain tensor in the case of large displacements are given by [6]

$$\varepsilon_r = \frac{\partial U}{\partial r} + \frac{1}{2}\left(\frac{\partial W}{\partial r}\right)^2 - z\frac{\partial^2 W}{\partial r^2}, \quad \varepsilon_\theta = \frac{U}{r} - \frac{z}{r}\frac{\partial W}{\partial r}. \tag{2}$$

2.2. The bending strain, membrane strain and kinetic energies of a circular plate

The total strain energy, V, of the circular plate is given as the sum of the strain energy due to bending (V_b) and the membrane strain energy induced by large deflections (V_m): $V = V_m + V_b$. In the case of axisymmetric vibrations, the bending strain energy is given by [37]

$$V_b = \pi D \int_0^a \left[\left(\frac{\partial^2 W}{\partial r^2} + \frac{1}{r}\frac{\partial W}{\partial r}\right)^2 - 2(1-\nu)\frac{1}{r}\frac{\partial W}{\partial r}\frac{\partial^2 W}{\partial r^2}\right] r\,\mathrm{d}r \tag{3}$$

in which, $D = Eh^3/(12(1-\nu^2))$ is the bending stiffness of the plate, and E and ν are Young's modulus and the Poisson ratio of the plate material. In the case of a clamped plate, the bending strain energy expression (3) can be shown, by using integration by parts and the boundary conditions, to simplify to

$$V_b = \pi D \int_0^a \left[\left(\frac{\partial^2 W}{\partial r^2}\right)^2 + \frac{1}{r^2}\left(\frac{\partial W}{\partial r}\right)^2\right] r\,\mathrm{d}r. \tag{4}$$

The expression for the membrane strain energy induced by large deflections for an axisymmetric circular plate is given by [37]

$$V_m = \frac{12\pi D}{h^2} \int_0^a [e_1^2 - 2(1-\nu)e_2] r\,\mathrm{d}r, \tag{5}$$

where $e_1 = [\partial U/\partial r + \frac{1}{2}(\partial W/\partial r)^2] + U/r$, and $e_2 = [\partial U/\partial r + \frac{1}{2}(\partial W/\partial r)^2]U/r$, are the midplane first and second strain invariants, respectively. An approximation has been adopted in the present work consisting of neglecting the contribution of the in-plane displacement U in the membrane strain energy expression. Such an assumption of neglecting the in-plane displacements in the non-linear strain energy has been made in Refs. [18,27] when calculating the first two non-linear mode

shapes of fully clamped rectangular plates. For the first mode shape, the range of validity of this assumption has been discussed in the light of the experimental and numerical results obtained for the non-linear frequency–amplitude dependence and the non-linear bending stress estimates obtained at large vibration amplitude [18,26]. For the second fully clamped rectangular plates non-linear mode shape, the assumption of zero in-plane displacements has led to results which were in good agreement with those given in Ref. [38], based on the hierarchical finite element method and including the in-plane displacements in the formulation. Therefore, it seemed reasonable to start, in the application to circular plates of the semi-analytical model presented in the above references, by adopting the assumption of neglecting in-plane displacement in the circular plate case, for calculating the non-linear mode shapes, and the associated frequencies, and the non-linear bending stress patterns for a reasonable range of vibration amplitudes, because it induces a great simplification in the theory, a significant reduction in the size of the non-linear algebraic system, and it allows, as will be shown in the present work, an easy direct analytical estimation of the higher basic function contribution to the non-linear transverse mode shapes. Further investigations could be carried out, taking into account the in-plane displacement U, in order to examine the effects of large vibration amplitudes on the membrane stress patterns for clamped circular plates. The assumption introduced above leads to

$$V_m = \frac{3\pi D}{h^2} \int_0^a \left(\frac{\partial W}{\partial r}\right)^4 r \, \mathrm{d}r. \tag{6}$$

The total strain energy, V, is then given by

$$V = \pi D \int_0^a \left[\left(\frac{\partial^2 W}{\partial r^2}\right)^2 + \frac{1}{r^2}\left(\frac{\partial W}{\partial r}\right)^2 + \frac{3}{h^2}\left(\frac{\partial W}{\partial r}\right)^4 \right] r \, \mathrm{d}r. \tag{7}$$

In most engineering applications of thin plates, rotatory and in-plane inertia effects can be neglected [39]. Thus, the kinetic energy T of the circular plate reduces to

$$T = \pi \rho h \int_0^a \left(\frac{\partial W}{\partial t}\right)^2 r \, \mathrm{d}r, \tag{8}$$

where ρ is the plate mass per unit volume.

2.3. Discretization of the total strain and kinetic energy expressions

If the space and time functions are supposed to be separable and harmonic motion is assumed, the transverse displacement W can be written as

$$W(r,t) = w(r)\sin(\omega t). \tag{9}$$

The spatial function $w(r)$ is expanded in the form of finite series of n basic functions $w_i(r)$ as

$$w(r) = a_i w_i(r) \tag{10}$$

in which the usual summation convention for repeated indices is used over the range $[1,n]$. The transverse displacement $W(r,t)$ is then given by

$$W(r,t) = a_i w_i(r)\sin(\omega t). \tag{11}$$

Discretization of the total strain and kinetic energy expressions is made by substituting the expression for $W(r,t)$ given in Eq. (11) into Eqs. (7) and (8), and rearranging. This leads to the following expressions:

$$V = \tfrac{1}{2} a_i a_j k_{ij} \sin^2(\omega t) + \tfrac{1}{2} a_i a_j a_k a_l b_{ijkl} \sin^4(\omega t), \tag{12}$$

$$T = \tfrac{1}{2} \omega^2 a_i a_j m_{ij} \cos^2(\omega t), \tag{13}$$

where m_{ij}, k_{ij} and b_{ijkl} are the mass tensor, the rigidity tensor and the non-linearity tensor, respectively, given by

$$m_{ij} = 2\pi\rho h \int_0^a w_i w_j r \, \mathrm{d}r,$$

$$k_{ij} = 2\pi D \int_0^a \left(\frac{\mathrm{d}^2 w_i}{\mathrm{d}r^2} \frac{\mathrm{d}^2 w_j}{\mathrm{d}r^2} + \frac{1}{r^2} \frac{\mathrm{d}w_i}{\mathrm{d}r} \frac{\mathrm{d}w_j}{\mathrm{d}r} \right) r \, \mathrm{d}r, \tag{14}$$

$$b_{ijkl} = \frac{6\pi D}{h^2} \int_0^a \frac{\mathrm{d}w_i}{\mathrm{d}r} \frac{\mathrm{d}w_j}{\mathrm{d}r} \frac{\mathrm{d}w_k}{\mathrm{d}r} \frac{\mathrm{d}w_l}{\mathrm{d}r} r \, \mathrm{d}r.$$

It appears from Eqs. (14) that the tensors m_{ij} and k_{ij} are symmetric, and that the fourth order tensor b_{ijkl} satisfies: $b_{ijkl} = b_{klij}$, and $b_{ijkl} = b_{jikl}$.

2.4. Formulation of the governing equations

The dynamic behaviour of the structure is governed by Hamilton's principle, which is symbolically written as

$$\delta \int_0^{2\pi/\omega} (V - T) \, \mathrm{d}t = 0. \tag{15}$$

Replacing T and V by their discretized expressions given above in the energy condition (15), integrating the time functions, calculating the derivatives with respect to the a_i's, and taking into account the properties of symmetry of the tensors mentioned above, leads to the following set of non-linear algebraic equations:

$$2a_i k_{ir} + 3a_i a_j a_k b_{ijkr} - 2\omega^2 a_i m_{ir} = 0, \quad r = 1, \ldots, n. \tag{16}$$

Eqs. (16) represent a set of n non-linear algebraic equations relating the n coefficients a_i and the frequency ω. So, there are $(n+1)$ unknowns and n equations. In order to complete the formulation, a further equation has to be added to Eqs. (16). As no dissipation is considered here, such an equation can be obtained by applying the principle of conservation of energy, which can be written as

$$V_{max} = T_{max}, \tag{17}$$

where V_{max} is the maximum value of the total strain energy obtained from Eq. (12) for $t = \pi/(2\omega)$, at which $T = 0$, and T_{max} is the maximum value of the kinetic energy obtained from Eq. (13), for $t = 0$, at which $V = 0$. Eq. (17) leads to the following expression for ω^2:

$$\omega^2 = (a_i a_j k_{ij} + a_i a_j a_k a_l b_{ijkl}) / (a_i a_j m_{ij}) \tag{18}$$

which has to be substituted in Eqs. (16) to obtain a system of n non-linear algebraic equations leading to the n contribution coefficients a_i, $i = 1$ to n. Adopting the solution procedure used in Ref. [17,18], the contribution coefficient a_{r_0} of the basic function corresponding to the desired mode r_0 is first fixed, and the other basic function contribution coefficients are calculated via numerical solution of the remaining $(n-1)$ non-linear algebraic equations:

$$2a_i k_{ir} + 3a_i a_j a_k b_{ijkr} - 2\omega^2 a_i m_{ir} = 0, \quad r \neq r_0. \tag{19}$$

The values obtained for a_i, for $i \neq r_0$, are then substituted into Eq. (18) to obtain the corresponding value of $\omega_{r_0}^2$.

2.5. Non-dimensional formulation

To simplify the analysis and the numerical treatment of the set of non-linear algebraic equations, non-dimensional formulation has been considered by putting the spatial displacement function as

$$w_i(r) = h w_i^*(r^*), \tag{20}$$

where $r^* = r/a$ is the non-dimensional radial co-ordinate.

Eqs. (19) can be rewritten in non-dimensional form as

$$2a_i k_{ir}^* + 3a_i a_j a_k b_{ijkr}^* - 2\omega^{*2} a_i m_{ir}^* = 0, \quad r \neq r_0, \tag{21}$$

where ω^* is the non-dimensional non-linear frequency parameter defined by

$$\omega^{*2} = \frac{\rho h a^4}{D}\omega^2 \tag{22}$$

in which ω^{*2} is given by the following expression:

$$\omega^{*2} = (a_i a_j k_{ij}^* + a_i a_j a_k a_l b_{ijkl}^*)/(a_i a_j m_{ij}^*). \tag{23}$$

The m_{ij}^*, k_{ij}^* and b_{ijkl}^* terms are non-dimensional tensors related to the dimensional ones by the following relationships:

$$m_{ij} = 2\pi\rho a^2 h^3 m_{ij}^*, \quad k_{ij} = \frac{2\pi D h^2}{a^2} k_{ij}^*, \quad b_{ijkl} = \frac{2\pi D h^2}{a^2} b_{ijkl}^*. \tag{24}$$

These non-dimensional tensors are defined by

$$m_{ij}^* = \int_0^1 w_i^* w_j^* r^* \, \mathrm{d}r^*,$$

$$k_{ij}^* = \int_0^1 \left(\frac{\mathrm{d}^2 w_i^*}{\mathrm{d}r^{*2}} \frac{\mathrm{d}^2 w_j^*}{\mathrm{d}r^{*2}} + \frac{1}{r^{*2}} \frac{\mathrm{d}w_i^*}{\mathrm{d}r^*} \frac{\mathrm{d}w_j^*}{\mathrm{d}r^*} \right) r^* \, \mathrm{d}r^*,$$

$$b_{ijkl}^* = 3 \int_0^1 \frac{\mathrm{d}w_i^*}{\mathrm{d}r^*} \frac{\mathrm{d}w_j^*}{\mathrm{d}r^*} \frac{\mathrm{d}w_k^*}{\mathrm{d}r^*} \frac{\mathrm{d}w_l^*}{\mathrm{d}r^*} r^* \, \mathrm{d}r^*. \tag{25}$$

The parameters m_{ij}^*, k_{ij}^* and b_{ijkl}^* given above depend only on the chosen basic functions w_i^* and their first and second derivatives. Also, it should be noticed that the non-linear frequency parameter ω^* does not depend on the Poisson ratio since none of the parameters m_{ij}^*, k_{ij}^* and b_{ijkl}^* is

a function of v, but the non-linear frequency itself depends on v, via the plate bending stiffness $D = Eh^3/(12(1-v^2))$, as shown in Eq. (22).

2.6. Bending stress expressions

In the light of the assumption of zero in-plane displacement, only the bending stresses can be calculated with a good accuracy. At the instant of maximum amplitude, i.e., $t = \pi/(2\omega)$, the surface bending strains ε_{br} and $\varepsilon_{b\theta}$, obtained for $z = h/2$, are given by

$$\varepsilon_{br} = -\frac{h}{2}\left(\frac{\mathrm{d}^2 w}{\mathrm{d}r^2}\right), \quad \varepsilon_{b\theta} = -\frac{h}{2}\left(\frac{1}{r}\frac{\mathrm{d}w}{\mathrm{d}r}\right). \tag{26}$$

By using the classical thin plate assumption of plane stress and Hooke's law, the surface radial and circumferential bending stresses are given by

$$\begin{aligned} \sigma_{br} &= -\frac{Eh}{2(1-v^2)}\left[\left(\frac{\mathrm{d}^2 w}{\mathrm{d}r^2}\right) + v\left(\frac{1}{r}\frac{\mathrm{d}w}{\mathrm{d}r}\right)\right], \\ \sigma_{b\theta} &= -\frac{Eh}{2(1-v^2)}\left[\left(\frac{1}{r}\frac{\mathrm{d}w}{\mathrm{d}r}\right) + v\left(\frac{\mathrm{d}^2 w}{\mathrm{d}r^2}\right)\right]. \end{aligned} \tag{27}$$

In terms of the non-dimensional parameters defined in the previous section, the non-dimensional surface bending stresses σ^*_{br} and $\sigma^*_{b\theta}$ can be defined by

$$\begin{aligned} \sigma^*_{br} &= -\frac{1}{2(1-v^2)}\left[\left(\frac{\mathrm{d}^2 w^*}{\mathrm{d}r^{*2}}\right) + v\left(\frac{1}{r^*}\frac{\mathrm{d}w^*}{\mathrm{d}r^*}\right)\right], \\ \sigma^*_{b\theta} &= -\frac{1}{2(1-v^2)}\left[\left(\frac{1}{r^*}\frac{\mathrm{d}w^*}{\mathrm{d}r^*}\right) + v\left(\frac{\mathrm{d}^2 w^*}{\mathrm{d}r^{*2}}\right)\right]. \end{aligned} \tag{28}$$

The relationship between the dimensional and non-dimensional bending stresses is

$$\sigma^* = \frac{\sigma a^2}{Eh^2} \tag{29}$$

which is valid for both dimensional and non-dimensional pairs of bending stresses defined by Eqs. (27) and (28).

3. Numerical results and discussion

3.1. Numerical details

The basic functions w_i^* to be used in the expansion series of w in Eq. (10) must satisfy the theoretical clamped boundary conditions, i.e., zero displacement and zero slope along the circular edge. Since the linear problem of free axisymmetric flexural vibration of a clamped circular plate has an exact analytical solution, the chosen basic functions w_i^* were taken as the linear free

oscillation mode shapes given by [12]

$$w_i^*(r*) = A_i\left[\mathrm{J}_0(\beta_i r^*) - \frac{\mathrm{J}_0(\beta_i)}{\mathrm{I}_0(\beta_i)}\mathrm{I}_0(\beta_i r^*)\right], \tag{30}$$

where β_i is the ith real positive root of the transcendental equation

$$\mathrm{J}_1(\beta)\mathrm{I}_0(\beta) + \mathrm{J}_0(\beta)\mathrm{I}_1(\beta) = 0 \tag{31}$$

in which J_n and I_n are, respectively, the Bessel and the modified Bessel functions of the first kind and of order n. The parameter β_i is related to the ith non-dimensional linear frequency parameter $(\omega_\ell^*)_i$ of the plate by

$$\beta_i^2 = (\omega_\ell^*)_i. \tag{32}$$

Numerical values of $(\omega_\ell^*)_i$ may be found in Ref. [40] and the first 10 values are given in Table 1. A_i is chosen such that

$$\int_0^1 {w_i^*}^2 r^* \,\mathrm{d}r^* = 1. \tag{33}$$

So, there are a set of orthonormal functions, and the mass tensor associated with the transverse displacement is given by

$$m_{ij}^* = \int_0^1 w_i^* w_j^* r^* \,\mathrm{d}r^* = \delta_{ij}, \tag{34}$$

where δ_{ij} is the Kronecker symbol delta.

The first six basic functions w_i^*, $i = 1, \ldots, 6$, are shown in Fig. 2. The parameters k_{ij}^* and b_{ijkl}^* of Eqs. (25) were computed numerically by using Simpson's rule with 160 steps in the range $[0, 1]$.

The set of non-linear algebraic Eqs. (21) has been solved numerically by using a routine, based on a hybrid method combining the steepest descent and Newton's methods, which does not require a very good initial estimate of the solution [41]. A step procedure, similar to that described in Refs. [17,18,22] for beams and rectangular plates, was adopted here for ensuring rapid convergence when varying the amplitude, which allowed solutions to be obtained with a quite reasonable number of iterations (an average of 25 and 44 iterations for five and eight non-linear algebraic equations, respectively). For the r_0th ($r_0 = 1$ or 2) non-linear mode shape, the first calculation was made in the neighbourhood of the linear solution by attributing a small numerical value a to the coefficient a_{r_0} of the basic function $w_{r_0}^*$. The resulting solution was used as an initial estimate for the following step corresponding to $a + \Delta a$. Thus, by choosing in each case the convenient value of the step Δa, the r_0th non-linear mode shape has been calculated at various

Table 1
Non-dimensional linear frequencies, $(\omega_\ell^*)_i = \beta_i^2$, associated with the axisymmetric modes of a clamped isotropic circular plate for $i = 1$–10

i	1	2	3	4	5	6	7	8	9	10
$(\omega_\ell^*)_i$	10.2158	39.7710	89.1040	158.1830	247.0050	355.568	483.872	631.914	799.702	987.216

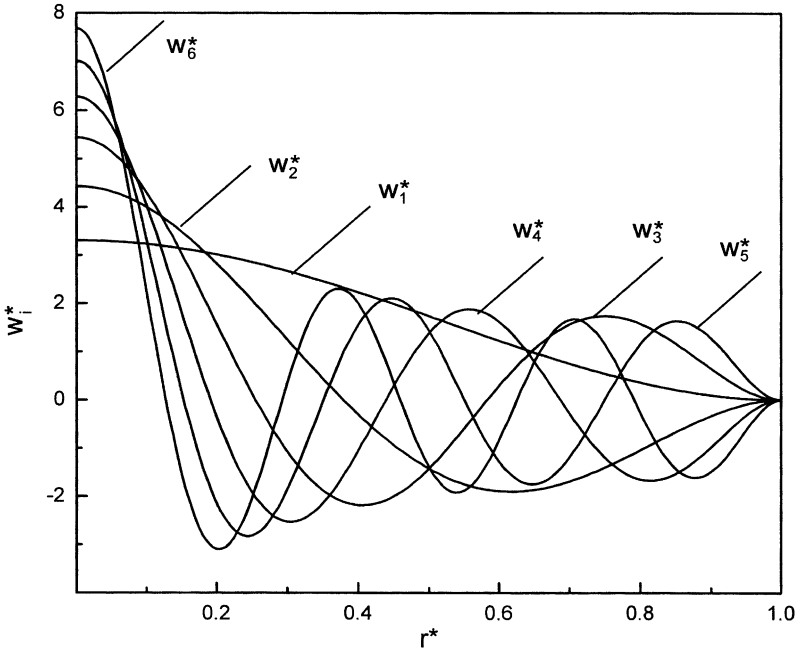

Fig. 2. Axisymmetric natural modes of vibration for a clamped circular plate w_i^* for $i = 1, \ldots, 6$.

maximum vibration amplitude to plate thickness ratios extending up to a given value. The limit of error residuals was imposed to be lower than 10^{-16} in all cases.

3.2. Convergence study of the spectral expansion

The convergence study of the spectral expansion used in the model is discussed here for the first and the second non-linear axisymmetric mode shapes. Tables 2(a) and (b) show the variation of the non-linear frequency ratios and the edge surface bending stresses associated to the first and the second non-linear axisymmetric mode shapes, respectively, with the number of basic functions used for a value of the non-dimensional amplitude obtained at the plate centre equal to 1.5. From these tables, it appears that accurate frequency and bending stress estimates may be achieved using six and nine basic functions in the spectral expansion for the first and second non-linear axisymmetric mode shapes, respectively.

3.3. General presentation of numerical results

To obtain, via the model presented above, the first and second non-linear axisymmetric mode shapes of a clamped circular plate, the first six and nine linear clamped circular plate axisymmetric eigenfunctions were used, respectively. Numerical results thus obtained are summarized in Tables 3(a) and (b). In Table 3(a), computed values of $a_2, \ldots, a_6$, obtained for some assigned values of a_1 varying from 0.005 up to 0.75, which correspond to a maximum non-dimensional vibration amplitude varying from 0.0165 to 2.3903, are given. Also, in Table 3(b), computed values of $a_1, a_3, a_4, \ldots, a_9$, corresponding to a_2 varying from 0.005 up to 0.50, which correspond to

Table 2
Convergence study of the spectral expansion for the first (a) and second (b) axisymmetric non-linear mode shapes for $w^*_{max} = 1.5$, where n is the number of basic functions used, $\omega^*_{n\ell}/\omega^*_{\ell}$ is the non-dimensional frequency ratio, and σ^*_{br} is the non-dimensional radial surface bending stress at the edge of the clamped circular plate ($\nu = 0.3$)

n	1	2	3	4	5	6	7	8	9	10
(a)										
$\omega^*_{n\ell}/\omega^*_{\ell}$	1.491	1.359	1.325	1.327	1.325	1.326	1.325	1.325		
$\lvert\sigma^*_{br}\rvert$	5.091	6.150	6.699	6.941	7.030	7.067	7.080	7.086		
(b)										
$\omega^*_{n\ell}/\omega^*_{\ell}$	1.644	1.401	1.394	1.392	1.378	1.375	1.376	1.373	1.374	1.373
σ^*_{br}	14.797	12.265	14.290	20.779	18.843	19.002	19.424	19.822	19.991	20.038

maximum non-dimensional vibration amplitudes varying from 0.0222 to 2.3862, are given. In each table, a_i represents the contribution of the ith basic function, w^*_{max} is the maximum non-dimensional amplitude, obtained at the plate centre, and $\omega^*_{n\ell}/\omega^*_{\ell}$ is the ratio of the non-linear non-dimensional frequency parameter defined in Eq. (23) to the corresponding linear non-dimensional frequency parameter given in Table 1. It can be seen from these tables that the non-linear non-dimensional frequencies calculated here from the non-linear analysis for very small values of a_1 and a_2, coincide exactly with the corresponding linear ones. Also, near to the linear frequency of a given mode, only the corresponding basic function has a significant contribution. At large vibration amplitudes, the higher order mode contributions and resonance frequencies increase with the amplitude of vibration.

3.4. Comparison of the amplitude–frequency dependence calculated via the present theory with previous results

In order to estimate the accuracy of the results obtained by the present theory and the effects of the approximations adopted, a comparison has been made with previous results. Such comparison was thought to lead to acceptable conclusions, especially with respect to the zero in-plane radial displacement assumption, since the non-linear resonant frequency depends on the non-linear strain energy due to the in-plane loads induced by large transverse displacements, and hence the importance of the terms neglected in the strain energy expression must be reflected in the non-linear frequency estimates. Also, further comparison concerning the amplitude dependence of the mode shapes and the associated bending stresses are made in the remainder of this paper. For clamped circular plates, most of the available published results are concerned with the first axisymmetric non-linear mode shape, and only one reference was found which deals with the second axisymmetric non-linear mode shape, which is mentioned below.

For the first axisymmetric non-linear mode shape numerical results, a detailed comparison was made between all of the results found in the literature and those obtained here [2,3,5,7–9,11,13–15,42,43]. Table 4(a) summarizes a set of results published during the period 1961–1986. As these results were based on various analytical assumptions and numerical solution techniques, a general comparison was made by calculating the average and the standard deviation of the non-linear frequency estimates obtained by various methods for each amplitude of vibration, as shown

Table 3
Contribution coefficients to the first (a) and second (b) non-linear axisymmetric mode shapes of the clamped isotropic circular plate, obtained numerically from iterative solution of the non-linear algebraic system (21)

w^*_{max}	$\omega^*_{n\ell}/\omega^*_{\ell}$	a_1	a_2	a_3	a_4	a_5	a_6	a_7	a_8	a_9
(a)										
0.0165	1.0000	0.005	−0.5336E − 07	0.1409E − 07	−0.4921E − 08	0.2242E − 08	−0.9836E − 09			
0.0331	1.0002	0.01	−0.3431E − 06	0.1079E − 06	−0.1288E − 07	0.5128E − 08	−0.2181E − 08			
0.0661	1.0008	0.02	−0.2595E − 05	0.8532E − 06	−0.4481E − 07	0.1274E − 07	−0.4853E − 08			
0.0992	1.0018	0.03	−0.8664E − 05	0.2863E − 05	−0.1149E − 06	0.2529E − 07	−0.8396E − 08			
0.1322	1.0032	0.04	−0.2041E − 04	0.6766E − 05	−0.2451E − 06	0.4613E − 07	−0.1336E − 07			
0.1653	1.0049	0.05	−0.3966E − 04	0.1318E − 04	−0.4598E − 06	0.7943E − 07	−0.2034E − 07			
0.3299	1.0194	0.10	−0.3070E − 03	0.1040E − 03	−0.3962E − 05	0.6780E − 06	−0.1171E − 06			
0.4935	1.0428	0.15	−0.9866E − 03	0.3435E − 03	−0.1608E − 04	0.3191E − 05	−0.4732E − 06			
0.6558	1.0739	0.20	−0.2195E − 02	0.7908E − 03	−0.4602E − 04	0.1051E − 04	−0.1528E − 05			
0.8168	1.1115	0.25	−0.3981E − 02	0.1490E − 02	−0.1059E − 03	0.2723E − 04	−0.4145E − 05			
0.9766	1.1547	0.30	−0.6338E − 02	0.2469E − 02	−0.2092E − 03	0.5939E − 04	−0.9736E − 05			
1.1354	1.2024	0.35	−0.9229E − 02	0.3742E − 02	−0.3686E − 03	0.1140E − 03	−0.2027E − 04			
1.2934	1.2537	0.40	−0.1260E − 01	0.5311E − 02	−0.5950E − 03	0.1983E − 03	−0.3819E − 04			
1.4508	1.3080	0.45	−0.1638E − 01	0.7166E − 02	−0.8968E − 03	0.3192E − 03	−0.6624E − 04			
1.6079	1.3647	0.50	−0.2053E − 01	0.9293E − 02	−0.1279E − 02	0.4828E − 03	−0.1073E − 03			
1.7646	1.4234	0.55	−0.2497E − 01	0.1167E − 01	−0.1745E − 02	0.6942E − 03	−0.1640E − 03			
2.0776	1.5455	0.65	−0.3460E − 01	0.1711E − 01	−0.2928E − 02	0.1274E − 02	−0.3348E − 03			
2.3903	1.6723	0.75	−0.4495E − 01	0.2329E − 01	−0.4431E − 02	0.2073E − 02	−0.5948E − 03			
(b)										
0.0222	1.0001	0.4431E − 06	0.005	−0.3608E − 06	0.3192E − 07	0.2079E − 07	0.1922E − 07	−0.1678E − 08	0.1052E − 08	0.2959E − 08
0.0443	1.0005	0.3591E − 05	0.01	−0.2847E − 05	0.1346E − 06	0.2258E − 06	0.1302E − 06	−0.1123E − 07	0.4114E − 08	0.5346E − 08
0.0886	1.0020	0.2853E − 04	0.02	−0.2258E − 04	0.8511E − 06	0.1919E − 05	0.9856E − 06	−0.8731E − 07	0.2480E − 07	0.5883E − 08
0.1329	1.0044	0.9562E − 04	0.03	−0.7561E − 04	0.2833E − 05	0.6527E − 05	0.3259E − 05	−0.3039E − 06	0.8197E − 07	−0.2140E − 08
0.1772	1.0078	0.2246E − 03	0.04	−0.1775E − 03	0.6956E − 05	0.1546E − 04	0.7580E − 05	−0.7567E − 06	0.2024E − 06	−0.2056E − 07
0.2215	1.0122	0.4335E − 03	0.05	−0.3424E − 03	0.1436E − 04	0.3006E − 04	0.1449E − 04	−0.1568E − 05	0.4232E − 06	−0.4875E − 07
0.4432	1.0467	0.3176E − 02	0.10	−0.2497E − 02	0.1625E − 03	0.2284E − 03	0.9867E − 04	−0.1726E − 04	0.5505E − 05	−0.1764E − 06
0.6668	1.0991	0.9485E − 02	0.15	−0.7406E − 02	0.7262E − 03	0.7014E − 03	0.2611E − 03	−0.7223E − 04	0.2995E − 04	−0.3258E − 06
0.8943	1.1651	0.1957E − 01	0.20	−0.1514E − 01	0.2052E − 02	0.1454E − 02	0.4553E − 03	−0.1857E − 03	0.1018E − 03	−0.4826E − 05
1.1275	1.2412	0.3309E − 01	0.25	−0.2534E − 01	0.4405E − 02	0.2399E − 02	0.6238E − 03	−0.3540E − 03	0.2538E − 03	−0.2671E − 04
1.3672	1.3253	0.4956E − 01	0.30	−0.3751E − 01	0.7906E − 02	0.3406E − 02	0.7301E − 03	−0.5534E − 03	0.5110E − 03	−0.8615E − 04
1.6135	1.4157	0.6848E − 01	0.35	−0.5118E − 01	0.1255E − 01	0.4342E − 02	0.7675E − 03	−0.7538E − 03	0.8833E − 03	−0.2044E − 03
1.8659	1.5113	0.8944E − 01	0.40	−0.6596E − 01	0.1823E − 01	0.5104E − 02	0.7516E − 03	−0.9299E − 03	0.1366E − 02	−0.3978E − 03
2.1236	1.6112	0.1121E + 00	0.45	−0.8152E − 01	0.2481E − 01	0.5626E − 02	0.7096E − 03	−0.1067E − 02	0.1946E − 02	−0.6749E − 03
2.3862	1.7150	0.1361E + 00	0.50	−0.9763E − 01	0.3214E − 01	0.5878E − 02	0.6706E − 03	−0.1160E − 02	0.2604E − 02	−0.1036E − 02

Table 4
(a) Frequency ratio $\omega^*_{n\ell}/\omega^*_{\ell}$ for various vibration amplitudes associated with the fundamental mode of clamped immovable circular plates for a Poisson's ratio $\nu = 0.3$; (b) Average and standard deviation of values given in (a)

(a)

w^*_{max}	Present work 2002	[2][a] 1961	[5][a] 1962	[8][b] 1963	[9][b] 1965	[11][b] 1971	[11][a] 1971	[3][a] 1972	[14][c] 1976	[7][a] 1977	[43][b] 1977	[13][c] 1981	[42][b] 1981	[42][a] 1981	[15][c] 1986	[15][a] 1986
0.2	1.0072	1.0070	1.0079	1.0084	1.0084	1.0075	1.0068	1.0070	1.0073	1.0075	1.0066	1.0081	—	—	1.0072	1.0050
0.4	1.0284	1.0278	1.0313	1.0331	1.0332	1.0298	1.0290	1.0278	1.0284	1.0296	1.0263	1.0285	—	—	1.0284	1.0198
0.5	1.0439	1.0431	1.0485	1.0512	1.0514	1.0462	1.0450	1.0431	—	1.0459	1.0408	—	1.0460	1.0434	—	—
0.6	1.0623	1.0614	1.0690	1.0728	1.0732	1.0659	1.0642	1.0614	1.0624	1.0654	1.0583	1.0624	—	—	1.0624	1.0441
0.8	1.1073	1.1065	1.1194	1.1258	1.1269	1.1145	1.1115	1.1065	1.1075	1.1135	1.1015	1.1075	—	—	1.1075	1.0770
1.0	1.1615	1.1617	1.1808	1.1902	1.1924	1.1740	1.1696	1.1617	1.1618	1.1724	1.1547	1.1618	1.1740	1.1647	1.1619	1.1179
1.5	1.3255	1.3343	1.3711	—	—	—	—	1.3343	—	1.3568	1.3229	—	1.3580	1.3405	—	—
2.0	1.5147	1.5423	1.5982	—	—	—	—	1.5424	—	1.5790	1.5275	—	1.5588	1.5361	—	—

(b)

w^*_{max}	Average	Standard deviation ($\times 10^2$)
0.2	1.0073	0.08
0.4	1.0287	0.31
0.5	1.0457	0.31
0.6	1.0632	0.67
0.8	1.1095	1.15
1.0	1.1663	1.63
1.5	1.3429	1.61
2.0	1.5499	2.57

[a] Formulations based on the von Kármán equations.
[b] Formulations based on the Berger hypothesis.
[c] Formulations based on the neglect of the in-plane deformation.

in Table 4(b). Good agreement can be noticed between the various results, and although the standard deviation increases with displacement amplitude, it remains within a reasonable range. For amplitudes up to twice the plate thickness, it does not exceed 2.57%. However, the results of Ref. [15], obtained by a finite element formulation in which a linearization function was used and in-plane deformation and in-plane inertia were taken into account, exhibits less hardening behaviour than the other results. In fact, this formulation has been shown to be erroneous in Ref. [44]. It can be seen also that the present results are very close to the average and to those of Ref. [2], in which the stress function approach was used and the solution, obtained using a one-term Galerkin procedure, was expressed in terms of elliptic functions.

For the second non-linear axisymmetric mode shape, the only reference found deals with the non-linear axisymmetric vibrations of a clamped circular plate with initial deflection and initial edge displacement [21]. In this reference, the stress function approach was used and the problem was considered to be well presented by a three-degree-of-freedom system. The solution of the problem was based on the Galerkin procedure and the harmonic balance method. The numerical results concerning the effect of the amplitude of vibration on the non-linear frequencies were given by considering the root mean square value (r.m.s.) of the dynamic response at the centre of the plate. Hence, in order to compare the present amplitude–frequency dependence corresponding to the second axisymmetric non-linear mode shape with that obtained in Ref. [21], the r.m.s. value of the maximum non-dimensional amplitude $(w^*_{max})_{r.m.s.}$ has been calculated. Fig. 3 shows a good agreement between results given in Ref. [21] and the results calculated via the present model, with a maximum discrepancy of 3% for a maximum value of the non-dimensional amplitude of 1.43 corresponding to an r.m.s. value of 1. The non-dimensional non-linear frequencies of Ref. [21] were read from graphs and correspond to the second non-linear mode shape backbone curve of a clamped circular plate with no initial deflection and no initial edge displacement (see Fig. 5 in this reference).

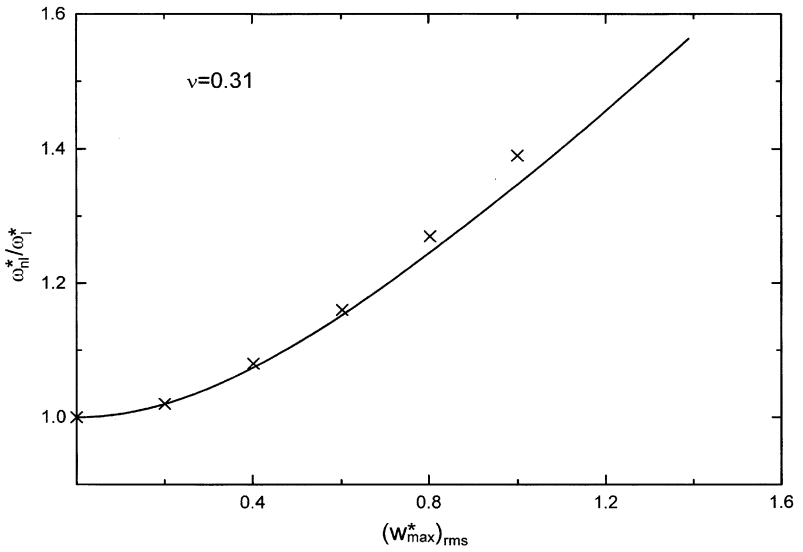

Fig. 3. Comparison of the non-dimensional frequency ratio of the second non-linear axisymmetric mode shape of a clamped circular plate. (×) values taken from Ref. [21]; — present work.

In the light of the above observations, it can be concluded that the assumption of zero in-plane displacement made in the expression of the membrane strain energy can lead to good estimation of the first two axisymmetric non-linear mode shapes of clamped circular plates for reasonable values of the vibration amplitudes. This justifies use of this assumption for such intervals of vibration amplitudes, since it makes the non-linear problem much easier to represent and to solve, and it leads to numerical and analytical results which may be considered to be of a sufficient accuracy for several engineering applications.

3.5. Amplitude–frequency dependence

The dependence of the non-linear frequency on the non-dimensional vibration amplitude is plotted in Fig. 4, for both the first and second non-linear axisymmetric mode shapes of a clamped circular plate and a hardening type of non-linearity is observed. Also, the curves show that the first non-linear mode shape exhibits less change in frequency with the vibration amplitude than does the second non-linear axisymmetric mode shape. Such a non-linear effect has been mentioned in Ref. [27] for the first two non-linear mode shapes of fully clamped rectangular plates, and was explained by the fact that the deflection shape associated with the first mode shape produces less induced tensile forces than does that associated with the second mode shape for the same maximum displacement amplitude.

3.6. Amplitude dependence of the first and second non-linear axisymmetric mode shapes of clamped circular plates

Most of the available results in the study of non-linear vibrations of clamped circular plates have been concerned with the determination of the so-called backbone curves, especially for the

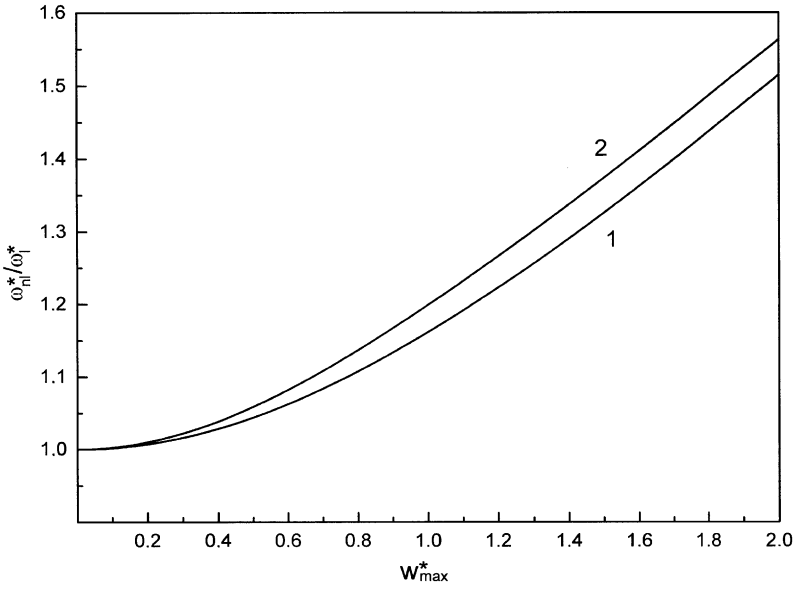

Fig. 4. Effects of large vibration amplitudes on the frequencies of the first (1) and second (2) non-linear axisymmetric mode shapes of a clamped circular plate.

fundamental non-linear mode shape. The advantage of the model used here is that it also gives the deformation of the mode shapes due to the geometrical non-linearity. This effect was illustrated in Ref. [6], in which Von Kármán equations and the Kantorovich method were used, by comparing the normalized linear fundamental mode shape to the non-linear one, for a non-dimensional amplitude of 2, and a significant difference was found. The normalized non-linear mode shape obtained in this reference and that obtained here are given in Fig. 5. It can be seen that both results are in a good agreement near to the clamped edge. However, some discrepancy is seen in the central part of the plate. The normalized first and second axisymmetric non-linear mode shapes are plotted in Figs. 6(a) and (b), respectively, for various values of the maximum non-dimensional amplitudes w^*_{max}. All curves show the amplitude dependence of the first and second axisymmetric non-linear mode shapes and an increase of curvatures near to the clamped edge, which may lead one to expect that the bending stress near the edge of the plate will increase nonlinearly with the increase of the vibration amplitude. This is examined in the next subsection.

3.7. *Analysis of the radial bending stress distribution associated with the first and second non-linear axisymmetric mode shapes*

The non-linear behaviour of non-dimensional surface radial bending stress distribution associated with the first and second axisymmetric non-linear mode shapes is depicted in Figs. 7 and 8. As mentioned previously, Figs. 7(a) and (b) show that the results obtained here for the radial bending stress associated with the first and second non-linear mode shapes at the clamped edge of the plate exhibit a higher increase with the vibration amplitude, compared with that

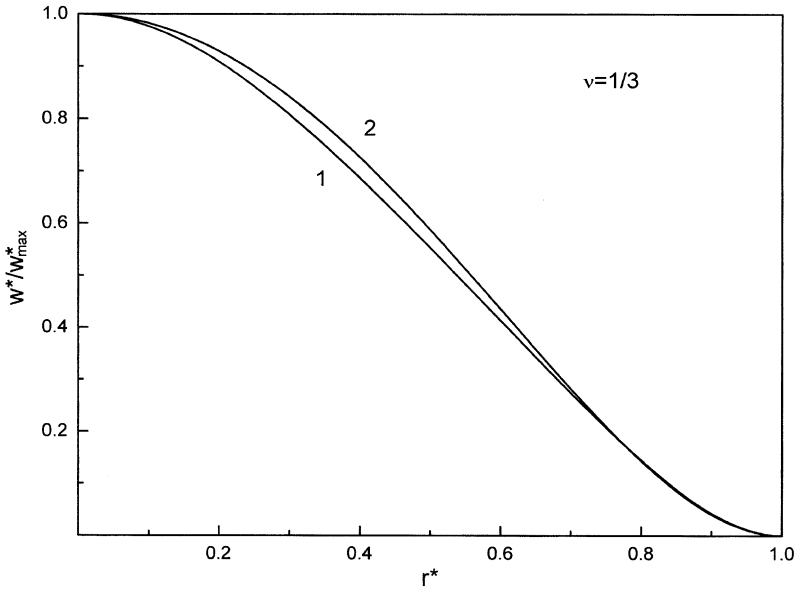

Fig. 5. Comparison of normalized fundamental non-linear mode shape of a clamped circular plate at a maximum non-dimensional vibration amplitude $w^*_{max} = 2.0$: (1) present solution; (2) solution from Ref. [6].

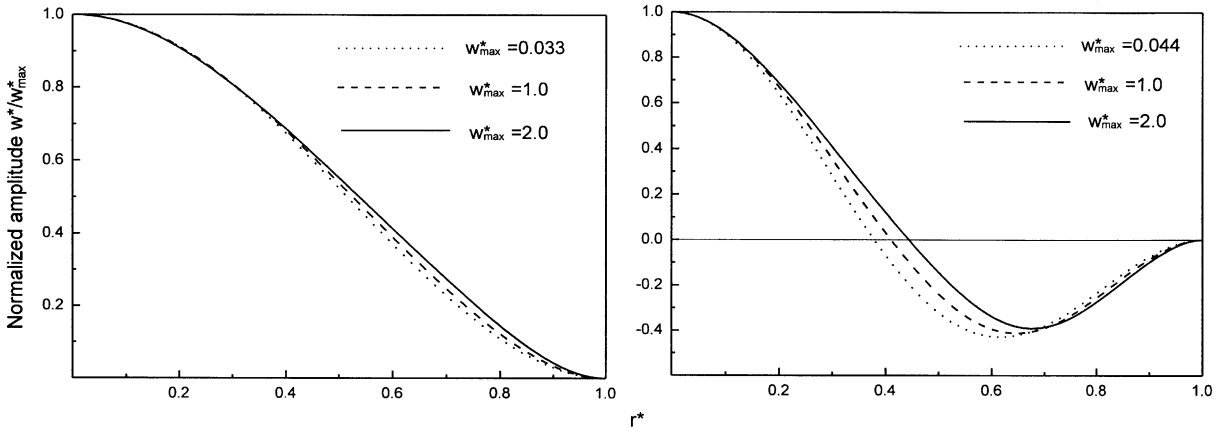

Fig. 6. Normalized radial sections of the first (a) and second (b) non-linear axisymmetric mode shapes of a clamped circular plate at various non-dimensional amplitudes w^*_{max}.

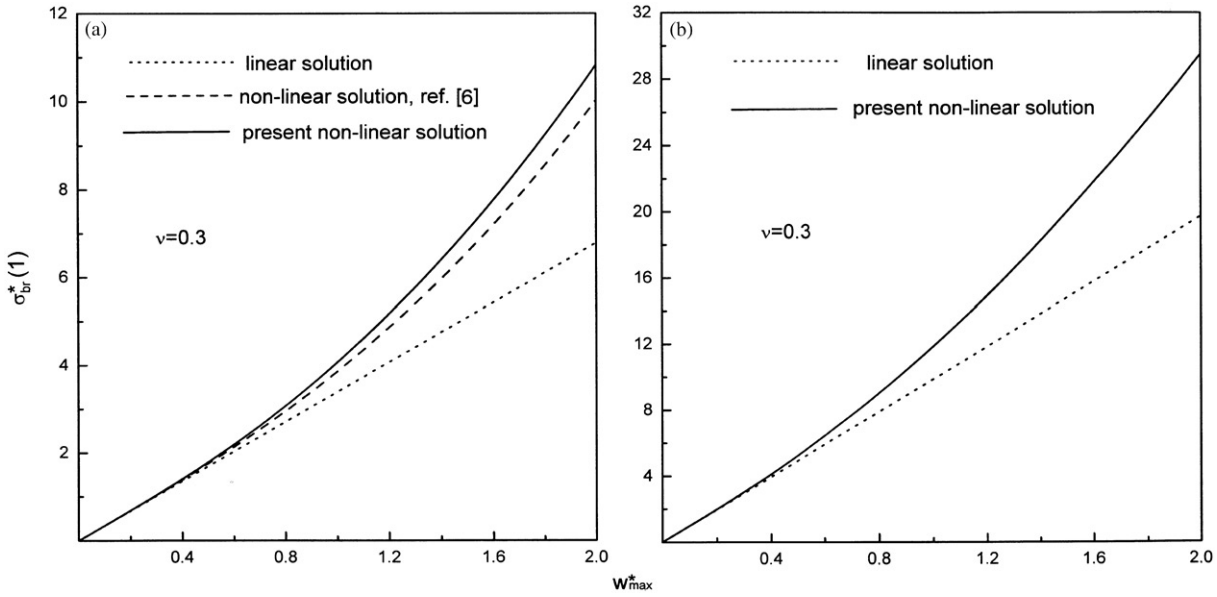

Fig. 7. Effect of large vibration amplitudes on the non-dimensional radial bending stress associated with the first (a) and second (b) non-linear axisymmetric mode shapes at the edge of the circular plate. Comparison with previous non-linear studies.

predicted by linear theory. The rate of increase in the radial bending stress is about twice the rate of increase expected in linear theory for the first mode, and about 1.8 for the second mode, when the maximum non-dimensional amplitude increases from 1.0 to 2.0. For the fundamental non-linear mode shape, the results concerning the bending stress at the clamped edge (Fig. 7(a)) are in good agreement with those given in Ref. [7], obtained by the same method as in Ref. [6] for the Poisson ratio $v = 0.3$, with a discrepancy not exceeding 5.8% for a maximum

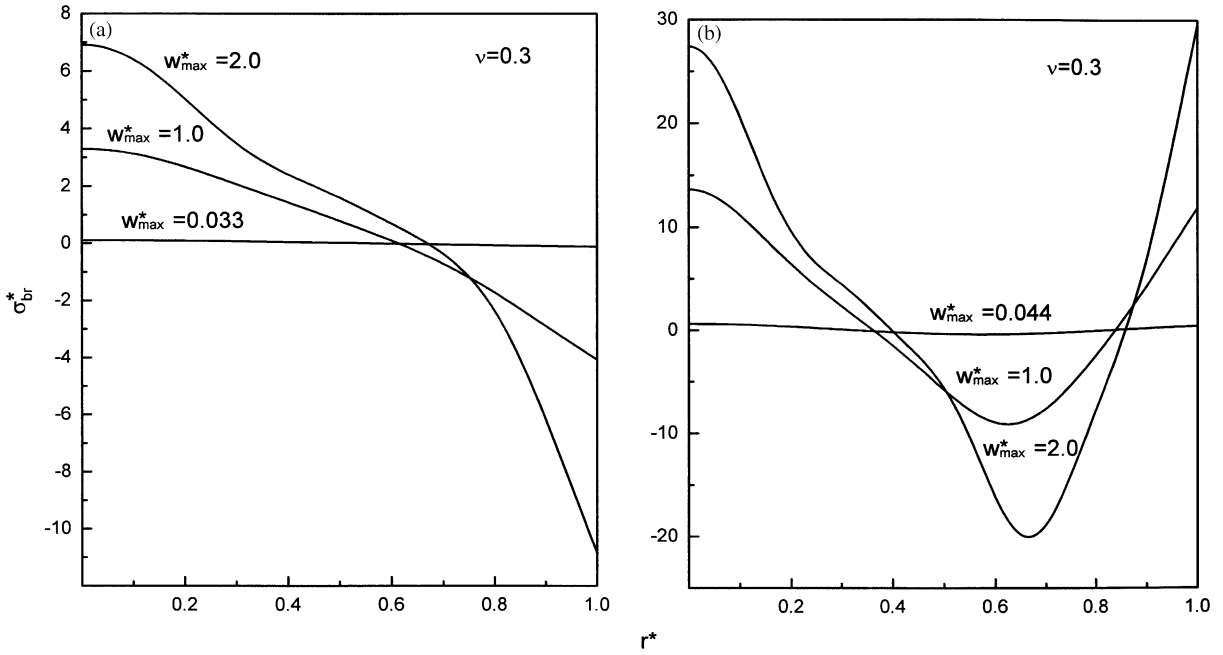

Fig. 8. Non-dimensional radial bending stress distribution associated with the clamped circular plate first (a) and second (b) non-linear axisymmetric mode shapes for various non-dimensional amplitudes w^*_{max}.

non-dimensional vibration amplitude of $w^*_{max} = 2$. The non-dimensional radial bending stress distributions associated with the first and second axisymmetric non-linear mode shapes are plotted in Figs. 8(a) and (b), respectively, for various values of the vibration amplitude. All curves show the amplitude dependence of the stress distribution, and exhibit a higher increase of the bending stress near to the clamped edge compared with that expected in linear theory. This behaviour is similar to that mentioned in Refs. [17,18,27] for the first three non-linear mode shapes of a clamped–clamped beam, and the first two non-linear mode shapes of fully clamped rectangular plates. In Fig. 9, the radial bending stress distribution associated with the first non-linear mode shape, obtained here for the Poisson ratio $v = \frac{1}{3}$ and a non-dimensional maximum vibration amplitude $w^*_{max} = 1.0$, is compared with the solution obtained in Ref. [6], in which the in-plane displacement is included in the model via the Airy stress function. It can be seen that the two curves are very close to each other. This is another check of the validity of the approximation of zero in-plane radial displacement made in the expression of the membrane strain energy used in the present model for vibration amplitudes of the order of at least once the plate thickness.

4. Explicit analytical solution and discussion

4.1. Approximate theory

The purpose of this section is to replace the iterative method of solution of the set of non-linear algebraic equations (21), necessary to obtain the clamped circular plate non-linear axisymmetric

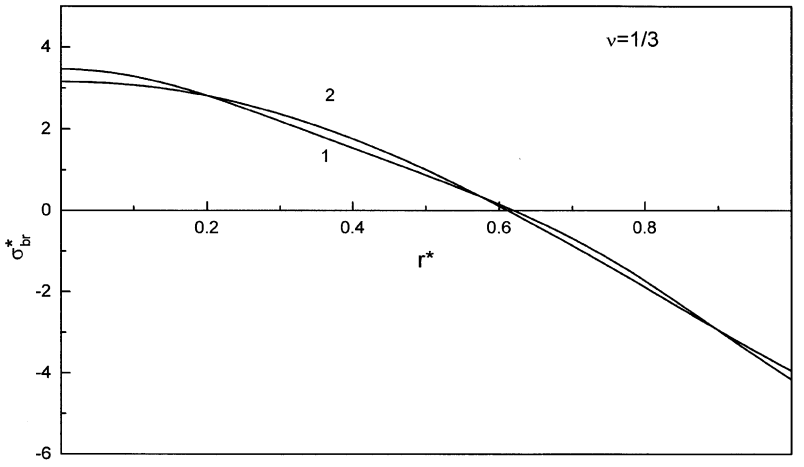

Fig. 9. Comparison of the non-dimensional radial bending stress distribution associated with the clamped circular plate first non-linear mode shape, for a non-dimensional vibration amplitude $w^*_{max} = 1.0$: (1) present solution; (2) solution from Ref. [6].

mode shapes and non-linear resonance frequencies at large vibration amplitudes, by an explicit approximate solution, which may be appropriate for engineering purposes, or for further analytical investigations. This explicit solution is obtained by applying and adapting the so-called first formulation developed for many beam and plate cases in Refs. [33–35]. A comparison is then made between the two solutions, i.e., iterative and analytical, in order to determine exactly the range of validity of the new approach. The main idea behind this approach is illustrated in Tables 3(a) and (b), in which data obtained via the numerical solution of the non-linear algebraic system (21) are presented for the first two non-linear axisymmetric mode shapes of the clamped circular plate. It can be seen from these tables that the contribution coefficient a_{r_0} ($r_0 = 1$ or 2) of the basic function corresponding to the r_0th mode shape remains predominant for the whole range of vibration amplitudes considered. So, the others basic function contribution coefficients (a_i; $i \neq r_0$) may be regarded as small compared to a_{r_0}, and denoted in what follows as ε_i. For the first non-linear mode shape, the new approach is based on an approximation which consists of neglecting in the expression for $a_i a_j a_k b^*_{ijkr}$, appearing in Eq. (21), both first and second order terms with respect to ε_i, i.e., terms of the type $a_1^2 \varepsilon_k b^*_{11kr}$ or of the type $a_1 \varepsilon_j \varepsilon_k b^*_{1jkr}$, so that the only remaining term is $a_1^3 b^*_{111r}$. This approximation is acceptable because the computed values of the non-linearity parameters b^*_{ijkl} defined in Eq. (25) are of the same magnitude. Thus, Eq. (21) becomes

$$(k^*_{ir} - \omega^{*2} m^*_{ir})\varepsilon_i + \tfrac{3}{2} a_1^3 b^*_{111r} = 0, \quad r = 2, \ldots, 6 \tag{35}$$

in which the repeated index i is summed over the range [1,6]. Since the use of linear clamped circular plate mode shapes as basic functions leads to diagonal mass and rigidity matrices, the above system permits one to obtain explicitly the unknown basic function contributions $\varepsilon_2, \ldots, \varepsilon_6$ corresponding to a given value of the assigned first basic function contribution a_1 as follows:

$$\varepsilon_r = -\frac{3a_1^3 b^*_{111r}}{2(k^*_{rr} - \omega^{*2} m^*_{rr})}, \quad r = 2, \ldots, 6. \tag{36}$$

The ε_r's, $r \neq 1$, depend on the known parameters m^*_{rr}, k^*_{rr}, b^*_{111r}, the assigned value a_1, and the non-linear frequency parameter ω^*. To express simply ω^* with an acceptable accuracy, is made of the single-function formula, obtained from Eq. (23) in which all of the a_i's, except a_1, are taken equal to zero:

$$\omega^{*2} = \frac{k^*_{11}}{m^*_{11}} + \frac{b^*_{1111}}{m^*_{11}} a_1^2. \tag{37}$$

In Fig. 10, the non-linear frequency estimates, calculated using the single-function formula (37) and the complete formula (23), are plotted against the maximum non-dimensional amplitude w^*_{max}. It can be seen from this figure that the single-mode approach gives a good estimate of the non-linear frequency parameter ω^{*2} for maximum plate displacement amplitudes up to once the plate thickness, with a percentage error below 1.2% compared with the exact one given by Eq. (23). Eq. (36) then becomes

$$\varepsilon_r = \frac{3a_1^3 b^*_{111r}}{2((k^*_{11} + a_1^2 b^*_{1111}) m^*_{rr}/m^*_{11} - k^*_{rr})}, \quad r = 2, \ldots, 6. \tag{38}$$

In the case considered here, the mass matrix is identical to the identity matrix, and Eq. (36) may be simplified to

$$\varepsilon_r = \frac{3a_1^3 b^*_{111r}}{2(k^*_{11} + a_1^2 b^*_{1111} - k^*_{rr})}, \quad r = 2, \ldots, 6. \tag{39}$$

Expression (39) is an explicit simple formula, allowing direct calculation of the higher mode contributions to the first non-linear clamped circular plate mode shape, as functions of the assigned first mode contribution a_1 and the known parameters k^*_{rr} and b^*_{111r} (given in Table 5),

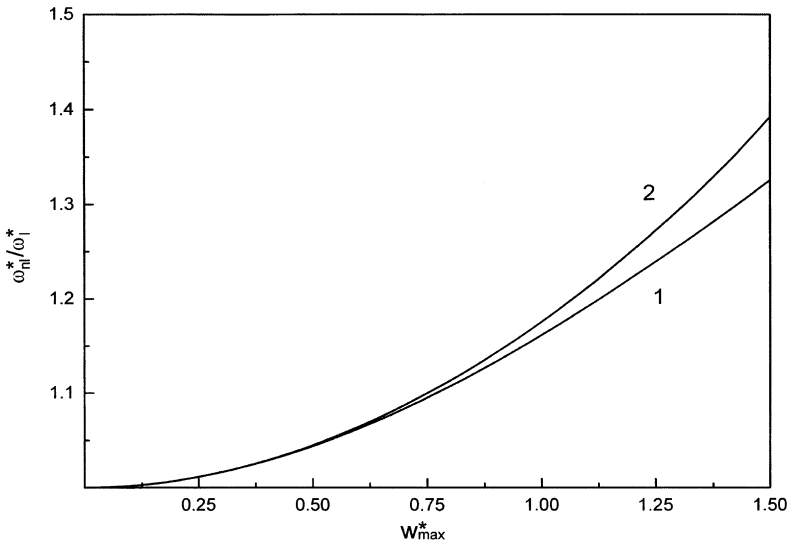

Fig. 10. Comparison of frequencies for the first non-linear clamped circular plate mode shape obtained by (1) non-linear algebraic equations; (2) explicit analytical solution.

Table 5
Numerical values of the clamped circular plate modal parameters used in Eqs. (40) and (41) for the first and second non-linear axisymmetric mode shapes, respectively

i	k_{ii}	b_{111i}	b_{222i}
1	104.36203354	413.43678551	3528.40519155
2	1581.72063613	314.99966725	15654.37275753
3	7939.49692150	−552.56304252	12009.50441352
4	25021.47533853	51.00034570	−1446.93403556
5	61010.75063949	−15.34284414	−9720.90257942
6	126427.64357913	5.97779208	−10173.83002533
7	234131.84218791	—	1603.51509425
8	399314.10116068	—	−695.04380343
9	639530.94960823	—	360.96734928

which defines the first non-linear amplitude-dependent clamped circular plate mode shape $w^*_{nl\,1}(r^*, a_1)$, for a given assigned value a_1, as a series involving the clamped circular plate modal parameters, depending on the first six axisymmetric clamped circular plate functions $w^*_1, w^*_2, \ldots, w^*_6$:

$$w^*_{nl\,1}(r^*, a_1) = a_1 w^*_1(r^*) + \frac{3a_1^3 b^*_{1112}}{2(k^*_{11} + a_1^2 b^*_{1111} - k^*_{22})} w^*_2(r^*) + \cdots + \frac{3a_1^3 b^*_{1116}}{2(k^*_{11} + a_1^2 b^*_{1111} - k^*_{66})} w^*_6(r^*) \tag{40}$$

in which the predominant term, proportional to the first linear mode shape, is $a_1 w^*_1(r^*)$, and the other terms, proportional to the higher linear mode shapes $w^*_2(r^*), \ldots, w^*_6(r^*)$, are the corrections due to the non-linearity.

Similarly, the second non-linear amplitude-dependent clamped circular plate axisymmetric mode shape $w^*_{nl\,2}(r^*, a_2)$, for an assigned value a_2 of the second function contribution, is given as a series involving the clamped circular plate modal parameters depending on the first nine axisymmetric clamped circular plate functions by

$$w^*_{nl\,2}(r^*, a_2) = \frac{3a_2^3 b^*_{2221}}{2(k^*_{22} + a_2^2 b^*_{2222} - k^*_{11})} w^*_1(r^*) + a_2 w^*_2(r^*) + \frac{3a_2^3 b^*_{2223}}{2(k^*_{22} + a_2^2 b^*_{2222} - k^*_{33})} w^*_3(r^*) + \cdots + \frac{3a_2^3 b^*_{2229}}{2(k^*_{22} + a_2^2 b^*_{2222} - k^*_{99})} w^*_9(r^*). \tag{41}$$

4.2. Presentation and discussion of the numerical results obtained by the explicit solution corresponding to the first two axisymmetric non-linear mode shapes of the clamped circular plate

Replacing in Eq. (40), the clamped circular plate modal parameters by their numerical values corresponding to the first non-linear mode shape of the clamped circular plate given in Table 5,

Table 6
Contribution coefficients to the first (a) and second (b) non-linear axisymmetric mode shapes of the clamped isotropic circular plate, calculated via explicit expressions obtained from application of the approximate analytical solution

(a)

w^*_{max}	$\omega^*_{n\ell}/\omega^*_{\ell}$	a_1	ε_2	ε_3	ε_4	ε_5	ε_6
0.0165	1.0000	0.005	−0.3998E − 07	0.1322E − 07	−0.3838E − 09	0.4723E − 10	−0.8873E − 11
0.0331	1.0002	0.01	−0.3198E − 06	0.1058E − 06	−0.3070E − 08	0.3779E − 09	−0.7098E − 10
0.0661	1.0008	0.02	−0.2559E − 05	0.8463E − 06	−0.2456E − 07	0.3023E − 08	−0.5679E − 09
0.0992	1.0018	0.03	−0.8638E − 05	0.2856E − 05	−0.8290E − 07	0.1020E − 07	−0.1917E − 08
0.1322	1.0032	0.04	−0.2048E − 04	0.6771E − 05	−0.1965E − 06	0.2418E − 07	−0.4543E − 08
0.1653	1.0049	0.05	−0.4001E − 04	0.1322E − 04	−0.3838E − 06	0.4723E − 07	−0.8873E − 08
0.3299	1.0196	0.10	−0.3207E − 03	0.1058E − 03	−0.3071E − 05	0.3779E − 06	−0.7098E − 07
0.4932	1.0436	0.15	−0.1086E − 02	0.3575E − 03	−0.1037E − 04	0.1275E − 05	−0.2396E − 06
0.6545	1.0763	0.20	−0.2588E − 02	0.8481E − 03	−0.2458E − 04	0.3024E − 05	−0.5679E − 06

(b)

w^*_{max}	$\omega^*_{n\ell}/\omega^*_{\ell}$	ε_1	a_2	ε_3	ε_4	ε_5	ε_6	ε_7	ε_8	ε_9
0.0222	1.0001	0.4477E − 06	0.005	−0.3542E − 06	0.1157E − 07	0.3067E − 07	0.1528E − 07	−0.1293E − 08	0.3277E − 09	−0.1061E − 09
0.0443	1.0005	0.3579E − 05	0.01	−0.2834E − 05	0.9260E − 07	0.2454E − 06	0.1222E − 06	−0.1034E − 07	0.2621E − 08	−0.8487E − 09
0.0886	1.0020	0.2854E − 04	0.02	−0.2269E − 04	0.7410E − 06	0.1963E − 05	0.9779E − 06	−0.8275E − 07	0.2097E − 07	−0.6790E − 08
0.1329	1.0044	0.9581E − 04	0.03	−0.7667E − 04	0.2502E − 05	0.6626E − 05	0.3301E − 05	−0.2793E − 06	0.7078E − 07	−0.2292E − 07
0.1772	1.0079	0.2255E − 03	0.04	−0.1821E − 03	0.5932E − 05	0.1571E − 04	0.7825E − 05	−0.6620E − 06	0.1678E − 06	−0.5432E − 07
0.2214	1.0123	0.4363E − 03	0.05	−0.3564E − 03	0.1159E − 04	0.3069E − 04	0.1528E − 04	−0.1293E − 05	0.3277E − 06	−0.1061E − 06
0.4411	1.0483	0.3239E − 02	0.10	−0.2905E − 02	0.9322E − 04	0.2460E − 03	0.1224E − 03	−0.1035E − 04	0.2622E − 05	−0.8489E − 06
0.6525	1.1057	0.9763E − 02	0.15	−0.1012E − 01	0.3173E − 03	0.8330E − 03	0.4137E − 03	−0.3496E − 04	0.8855E − 05	−0.2866E − 05

leads to the following explicit expression:

$$w^*_{nl\,1}(r^*, a_1) = a_1 w^*_1(r^*) + \frac{945.0a_1^3}{(208.72 + 826.87a_1^2 - 3163.44)} w^*_2(r^*) - \frac{1659.69a_1^3}{(208.72 + 826.87a_1^2 - 15878.99)} w^*_3(r^*) + \frac{153a_1^3}{(208.72 + 826.87a_1^2 - 50042.95)} w^*_4(r^*) - \frac{46.03a_1^3}{(208.72 + 826.87a_1^2 - 122021.50)} w^*_5(r^*) + \frac{17.93a_1^3}{(208.72 + 826.87a_1^2 - 252855.29)} w^*_6(r^*). \quad (42)$$

In Table 6(a), numerical results for modal contributions to the first non-linear mode shape of a clamped circular plate, calculated here via the explicit expression (42), are summarized. The results given correspond to the values of $\varepsilon_2, \ldots, \varepsilon_6$ obtained for some assigned values of a_1 varying from 0.005 to 0.20, which correspond to maximum non-dimensional vibration amplitudes at the plate centre varying from 0.0165 to 0.6545. For each solution, the corresponding values of $\omega^*_{n\ell}/\omega^*_\ell$ and w^*_{max} are also given. Comparison between Tables 6(a) and 3(a) shows that the higher mode contributions to the first non-linear clamped circular plate mode shape obtained from the explicit expressions (42) are very close to those calculated via iterative solution of the set of non-linear algebraic equations (21), corresponding to the first mode shape, i.e., $r_0 = 1$, for finite amplitudes of vibration up to 0.5 times the plate thickness, which corresponds to $a_1 \approx 0.15$. For higher values of the vibration amplitude, slight differences start to appear and increase with the amplitude of vibration. This may be seen in Figs. 11–15, in which the higher mode contributions obtained by the explicit approximate solution are plotted against the maximum non-dimensional vibration amplitude and compared with the iterative solution. To have an accurate conclusion concerning the limit of validity of the explicit approximate solution in engineering applications, a criterion was adopted, based on the effect of the differences appearing in the estimated basic function contributions to physical quantities, such as the non-linear frequency and the maximum bending stress obtained at the clamped edge of the circular plate. It was found, as may be seen in Figs. 10 and 16, that for vibration amplitudes up to the plate thickness, the error induced by the approximate explicit solution does not exceed 1.2% for the non-linear frequency, and 4.5% for the maximum associated non-linear bending stress at the clamped edge.

Replacing now in Eq. (41), the clamped circular plate modal parameters by their numerical values (given in Table 5) corresponding to the second non-linear axisymmetric mode shape of the clamped circular plate, leads to the following explicit expression:

$$w^*_{nl\,2}(r^*, a_2) = \frac{10585.22a_2^3}{(3163.44 + 31308.75a_2^2 - 208.72)} w^*_1(r^*) + a_2 w^*_2(r^*) + \frac{36028.51a_2^3}{(3163.44 + 31308.75a_2^2 - 15878.99)} w^*_3(r^*)$$

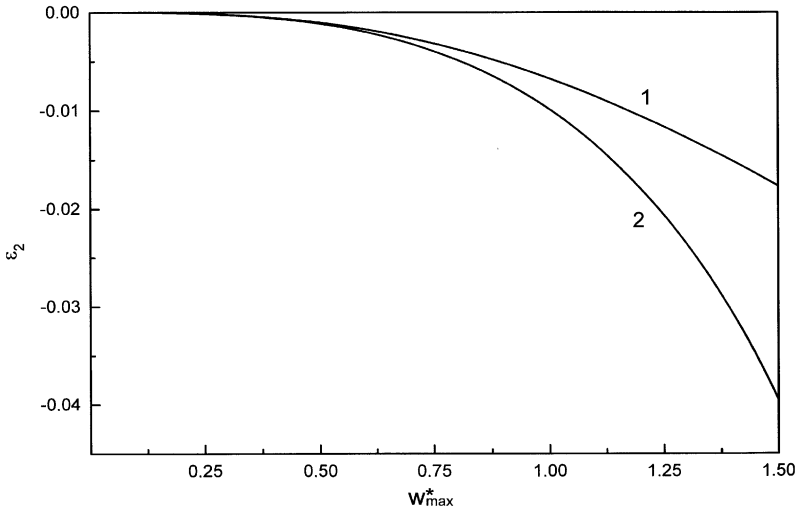

Fig. 11. Comparison between the values of the modal contribution ε_2 of the first non-linear mode shape of a clamped circular plate. Key as for Fig. 10.

$$
\begin{aligned}
&- \frac{4340.80a_2^3}{(3163.44 + 31308.75a_2^2 - 50042.95)} w_4^*(r^*) \\
&- \frac{29162.71a_2^3}{(3163.44 + 31308.75a_2^2 - 122021.50)} w_5^*(r^*) \\
&- \frac{30521.49a_2^3}{(3163.44 + 31308.75a_2^2 - 252855.29)} w_6^*(r^*) \\
&+ \frac{4810.55\,a_2^3}{(3163.44 + 31308.75\,a_2^2 - 468263.68)} w_7^*(r^*) \\
&- \frac{2085.13a_2^3}{(3163.44 + 31308.75a_2^2 - 798628.20)} w_8^*(r^*) \\
&+ \frac{1082.90a_2^3}{(3163.44 + 31308.75a_2^2 - 1279061.90)} w_9^*(r^*). \qquad (43)
\end{aligned}
$$

In Table 6(b), numerical results for modal contributions to the second axisymmetric non-linear mode shape of a clamped circular plate, calculated here via the explicit expression (43), are summarized. The results given correspond to the values of ε_1, ε_3, $\varepsilon_4, \ldots, \varepsilon_9$ obtained for some assigned values of a_2 varying from 0.005 to 0.15, which correspond to maximum non-dimensional vibration amplitudes at the plate centre varying from 0.0222 to 0.6525. For each solution, the corresponding values of $\omega_{n\ell}^*/\omega_\ell^*$ and w_{max}^* are also given. Comparison between Tables 6(b) and 3(b) shows that the higher mode contributions to the second axisymmetric non-linear clamped circular plate mode shape obtained from the explicit expressions (43) are very close to those calculated via solution of the set of non-linear algebraic equations (21), corresponding to the second axisymmetric non-linear mode shape, i.e., $r_0 = 2$, for finite amplitudes of vibration up to

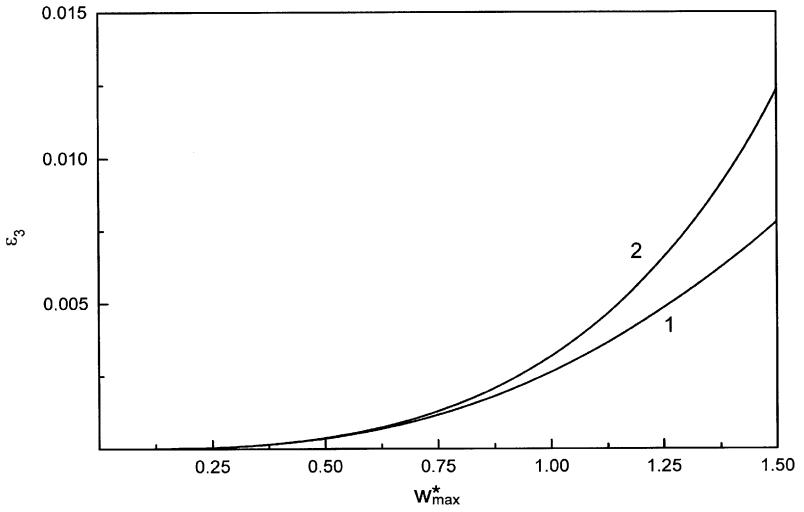

Fig. 12. Comparison between the values of the modal contribution ε_3 of the first non-linear mode shape of a clamped circular plate. Key as for Fig. 10.

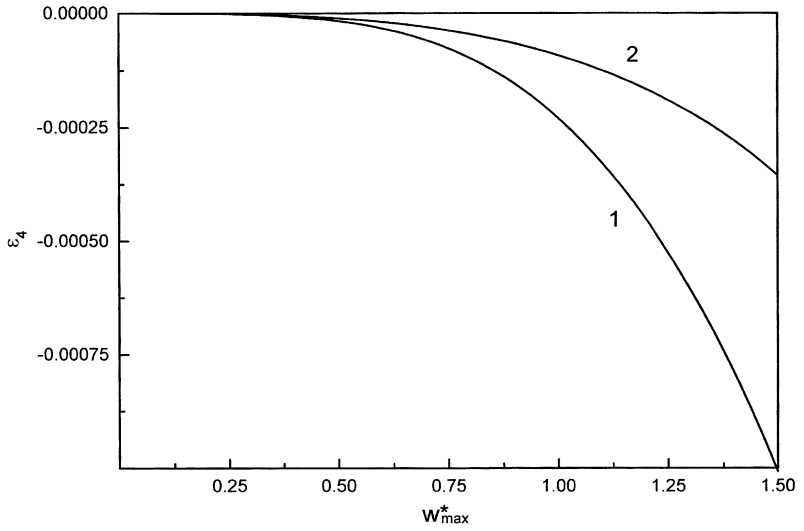

Fig. 13. Comparison between the values of the modal contribution ε_4 of the first non-linear mode shape of a clamped circular plate. Key as for Fig. 10.

0.44 times the plate thickness, which corresponds to $a_2 \approx 0.10$. For higher values of the vibration amplitude, slight differences start to appear and increase with the amplitude of vibration.

5. Conclusions

The non-linear axisymmetric free vibration of a clamped thin isotropic circular plate has been examined by a theoretical model developed in Ref. [22] for non-linear free vibrations of thin

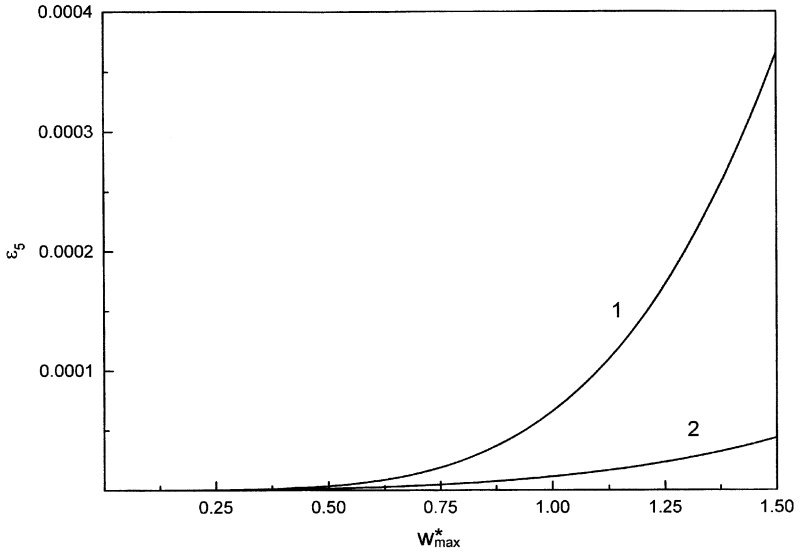

Fig. 14. Comparison between the values of the modal contribution ε_5 of the first non-linear mode shape of a clamped circular plate. Key as for Fig. 10.

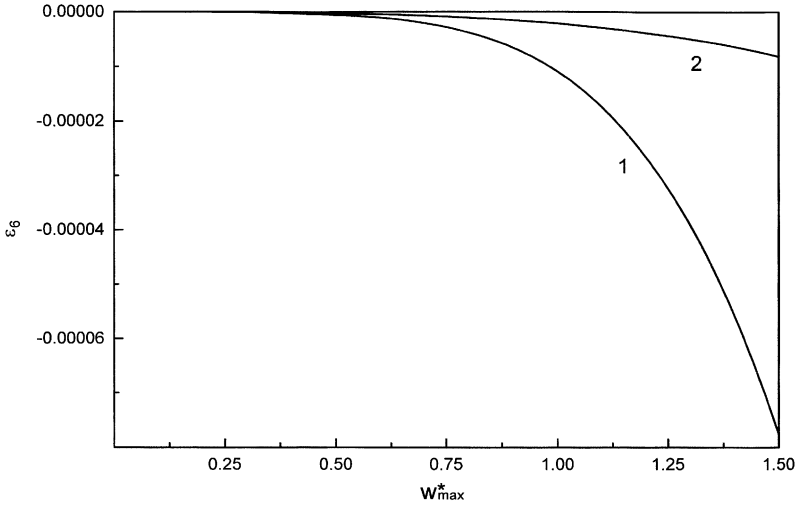

Fig. 15. Comparison between the values of the modal contribution ε_6 of the first non-linear mode shape of a clamped circular plate. Key as for Fig. 10.

elastic structures occurring at large displacement amplitudes, in order to determine the effects of large vibration amplitudes on the first and second axisymmetric mode shapes and their corresponding natural frequencies and bending stress distributions. Similar to the case of beams and rectangular plates [17,18,27], the theory reduces the non-linear free vibration problem to solution of a set of non-linear algebraic equations depending on the classical rigidity and mass tensors, and a non-linear term in which a fourth order tensor appears due to the geometrical non-linearity. The amplitude dependent first and second axisymmetric non-linear mode shapes were,

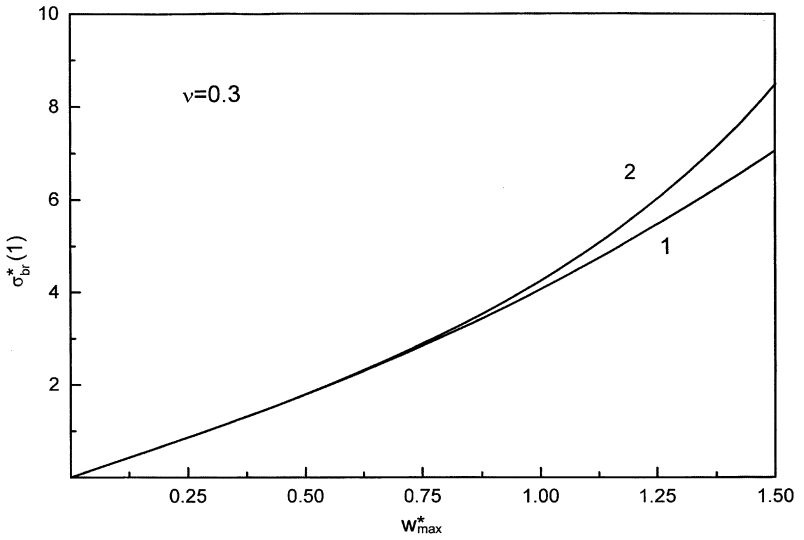

Fig. 16. Comparison between values of the radial bending stress at $r^* = 1$ for the first non-linear clamped circular plate mode shape. Key as for Fig. 10.

respectively, expressed as a series of six and nine clamped circular plate functions (linear mode shapes of free vibration expressed in terms of Bessel's functions).

Considering the results obtained, numerical data corresponding to various vibration amplitudes for the first and second axisymmetric non-linear mode shapes are given. The backbone curves obtained show a hardening type non-linearity (i.e., the frequency increases with increasing vibration amplitude). However, the first non-linear mode shape exhibits less change in frequency than does the second axisymmetric non-linear mode shape. Results obtained here for the amplitude–frequency dependence for the first non-linear mode shape are in good agreement with previous available results, in spite of the assumption of zero in-plane displacement adopted here. It was also shown that the geometrical non-linearity induces a deformation of the first two axisymmetric mode shapes and consequently, the rate of increase in the induced bending stresses at the clamped edge for the first and second mode shapes are 100% and 80%, respectively, higher than that predicted in the linear theory when the maximum non-dimensional vibration amplitude increases from 1 to 2. Also, the results obtained here for the radial bending stress associated with the first non-linear mode at the edge of the plate are in good agreement with those obtained in Ref. [7], in which the dynamic analogues of Von Kármán equations were used and solutions were obtained, based on the Kantorovich averaging method. However, the in-plane displacement must be taken into account in further investigations for a complete study of the geometrically non-linear free vibrations of clamped circular plates in order to permit accurate determination of both the bending and the membrane stress distributions. This work is actually in progress and will be presented in Part II of this series of papers.

In order to obtain explicit analytical solutions for the first two non-linear axisymmetric mode shapes of clamped circular plates, which are expected to be very useful in engineering applications and in further analytical developments, the improved version of the semi-analytical model

developed in Refs. [33–35] for beams and rectangular plates, has been adapted here to the case of clamped circular plates, leading to explicit expressions for the higher basic function contributions, which are shown to be in a good agreement with the iterative solutions, for maximum non-dimensional vibration amplitudes of 0.5 and 0.44 for the first and second axisymmetric non-linear mode shapes, respectively.

It appears from the present work that the non-linear model developed in Ref. [22], and its improved version presented in Refs. [33–35], allow the fundamental and higher order non-linear axisymmetric clamped circular plate mode shapes to be estimated quite easily. It has been shown also both qualitatively and quantitatively how it can be inaccurate to assume linear mode shapes when expressing the non-linear response of plate structures. Further investigations are needed to examine the non-linear forced response of clamped circular plates, and the effect of the in-plane displacement at very high vibration amplitudes.

Appendix A. Nomenclature

r, θ, z	cylindrical co-ordinates
U, W	in-plane and out-of-plane displacements of the middle plane point $(r, \theta, 0)$, respectively
u_r, u_θ, u_z	displacements along r, θ and z directions, respectively
ε_r, ε_θ	radial and circumferential strains
V_b, V_m, V	bending, membrane and total strain energy, respectively
E	Young's modulus
v	the Poisson ratio of the plate material
ρ	mass per unit volume of the plate material
a, h	radius and thickness of the circular plate, respectively
D	bending stiffness of the plate, $= Eh^3/12(1-v^2)$
e_1, e_2	midplane first and second strain invariants, respectively
T	kinetic energy of the plate
$w(r)$	transverse spatial function, $W(r,t) = w(r)\sin(\omega t)$
a_i	contribution coefficient of the ith basic function: $w(r) = a_i w_i(r)$
k_{ij}, m_{ij}, b_{ijkl}	general terms of the rigidity tensor, the mass tensor and the non-linearity tensor, respectively
ω	frequency parameter
ε_{br}, $\varepsilon_{b\theta}$	radial and circumferential surface bending strains
σ_{br}, $\sigma_{b\theta}$	radial and circumferential surface bending stresses
β_i	the ith eigenvalue parameter for a clamped axisymmetric circular plate
$(\omega_\ell^*)_i$	the ith non-dimensional linear natural frequency of axisymmetric vibrations of clamped circular plates: $(\omega_\ell^*)_i = \beta_i^2$
$w_i^*(r^*)$	the ith linear axisymmetric mode shape of a clamped circular plate
w_{max}^*	maximum non-dimensional vibration amplitude
$(w_{max}^*)_{r.m.s.}$	r.m.s. value of the maximum non-dimensional vibration amplitude
ε_i	contribution coefficient of the ith basic function, $\varepsilon_i = a_i$, for $i \neq r_0$, where r_0 is the order of the non-linear mode shape considered

$w^*_{nli}(r^*, a_i)$ the ith clamped circular plate non-linear mode shape for a given assigned value a_i of the ith function contribution star exponent indicates non-dimensional parameters

References

[1] G. Herrmann, Influence of large amplitudes on flexural motions of elastic plates, NACA TN 3578, 1955.
[2] N. Yamaki, Influence of large amplitudes on flexural vibrations of elastic plates, Zeitschrift für Angewandte Mathematik und Mechanik 41 (1961) 501–510.
[3] G.C. Kung, Y.H. Pao, Non-linear flexural vibrations of a clamped circular plate, Journal of Applied Mechanics, Transactions of the American Society of Mechanical Engineers 39 (1972) 1050–1054.
[4] M. Sathyamoorthy, Influence of transverse shear and rotatory inertia on non-linear vibrations of circular plates, Computers and Structures 60 (1996) 613–618.
[5] J.L. Nowinski, Non-linear transverse vibrations of circular elastic plates built-in at the boundary, Proceedings of the Fourth U.S. National Congress on Applied Mechanics, Vol. 1, 1962, pp. 325–334.
[6] C.L. Huang, B.E. Sandman, Large amplitude vibrations of rigidly clamped circular plates, International Journal of Nonlinear Mechanics 6 (1971) 451–468.
[7] C.L.D. Huang, I.M. Al-Khattat, Finite amplitude vibrations of a circular plate, International Journal of Nonlinear Mechanics 12 (1977) 297–306.
[8] T. Wah, Vibration of circular plates at large amplitudes, Proceedings of the American Society of Civil Engineers, Journal of Engineering Mechanics Division 89 (1963) 1–5.
[9] A.V. Srinivasan, Large amplitude free oscillations of beams and plates, American Institute of Aeronautics and Astronautics Journal 3 (1965) 1951–1953.
[10] H.M. Berger, A new approach to the analysis of large deflections of plates, Journal of Applied Mechanics, Transactions of the American Society of Mechanical Engineers 22 (1955) 465–472.
[11] T.W. Lee, P.T. Blotter, D.H.Y. Yen, On the non-linear vibrations of a clamped circular plate, Developments in Mechanics 6 (1971) 907–920.
[12] S. Sridhar, D.T. Mook, A.H. Nayfeh, Non-linear resonances in the forced responses of plates, Part I: symmetric responses of circular plates, Journal of Sound and Vibration 41 (1975) 359–373.
[13] J.N. Reddy, C.L. Huang, Large amplitude free vibrations of annular plates of variable thickness, Journal of Sound and Vibration 79 (1981) 387–396.
[14] G.V. Rao, K.K. Raju, I.S. Raju, Finite element formulation for the large amplitude free vibrations of beams and orthotropic circular plates, Journal of Sound and Vibration 6 (1976) 169–172.
[15] K. Decha-Umphai, C. Mei, Finite element method for non-linear forced vibrations of circular plates, International Journal for Numerical Methods in Engineering 23 (1986) 1715–1726.
[16] L. Azrar, R. Benamar, R.G. White, A semi-analytical approach to the non-linear dynamic response. Problem of S–S and C–C beams at large vibration amplitudes. Part I: general theory and application to the single mode approach to free and forced vibration analysis, Journal of Sound and Vibration 224 (2) (1999) 377–395.
[17] R. Benamar, M.M.K. Bennouna, R.G. White, The effects of large vibration amplitudes on the mode shapes and natural frequencies of thin elastic structures, part I: simply supported and clamped–clamped beams, Journal of Sound and Vibration 149 (1991) 179–195.
[18] R. Benamar, M.M.K. Bennouna, R.G. White, The effects of large vibration amplitudes on the mode shapes and natural frequencies of thin elastic structures, part II: fully clamped rectangular isotropic plates, Journal of Sound and Vibration 164 (1991) 399–424.
[19] A.W. Leissa, Non-linear analysis of plate and shell vibrations, International Conference on Recent Advances in Structural Dynamics, Proceedings, Vol. 1, University of Southampton, UK, 1984, pp. 241–260.
[20] M. Sathyamoorthy, M.E. Prasad, Multiple-mode non-linear analysis of circular plates, Proceedings of the American Society of Civil Engineers, Journal of Engineering Mechanics Division 109 (1983) 1114–1123.

[21] N. Yamaki, K. Otomo, M. Chiba, Non-linear vibrations of a clamped circular plate with initial deflection and initial edge displacement, part I: theory, Journal of Sound and Vibration 79 (1981) 23–42.
[22] R. Benamar, Non-linear Dynamic Behaviour of Fully Clamped Beams and Rectangular Isotropic and Laminated Plates, Ph.D. Thesis, Institute of Sound and Vibration Research, 1990.
[23] R.G. White, Comparison of some statistical properties of responses of aluminium alloy and cfrp plates to acoustic excitation, Composites 9 (1978) 251–258.
[24] C.E. Teh, Dynamic Behaviour and Acoustic Fatigue of Isotropic and Anisotropic Panels under Combined Acoustic Excitation and Static In-plane Compression, Ph.D. Thesis, Institute of Sound and Vibration Research, 1989.
[25] L. Azrar, R. Benamar, R.G. White, A semi-analytical approach to the non-linear dynamic response problem of beams at large vibration amplitudes, part II: Multimode approach to the forced vibration analysis, Journal of Sound and Vibration 255 (2002) 1–41.
[26] R. Benamar, M.M.K. Bennouna, R.G. White, The effects of large vibration amplitudes on the mode shapes and natural frequencies of thin elastic structures, part III: fully clamped rectangular isotropic plates—measurements of the mode shape amplitude dependence and the spatial distribution of harmonic distortion, Journal of Sound and Vibration 175 (1994) 377–395.
[27] M. El Kadiri, R. Benamar, R.G. White, The non-linear free vibration of fully clamped rectangular plates: second non-linear mode for various plate aspect ratios, Journal of Sound and Vibration 228 (2) (1999) 333–358.
[28] B. Harras, R. Benamar, R.G. White, Geometrically non-linear free vibration of fully clamped symmetrically laminated rectangular composite plates, Journal of Sound and Vibration 251 (4) (2002) 579–619.
[29] B. Harras, R. Benamar, R.G. White, Experimental and theoretical investigation of the linear and non-linear dynamic behaviour of a glare 3 hybrid composite panel, Journal of Sound and Vibration 252 (2) (2002) 281–315.
[30] F. Moussaoui, R. Benamar, R.G. White, The effects of large vibration amplitudes on the mode shapes and natural frequencies of thin elastics shells. Part I: coupled transverse-circumferential mode shapes of isotropic circular cylindrical shells of infinite length, Journal of Sound and Vibration 232 (5) (2000) 917–943.
[31] F. Moussaoui, R. Benamar, R.G. White, The effects of large vibration amplitudes on the mode shapes and natural frequencies of thin elastics shells. Part II: a new approach for free transverse constrained vibration of circular cylindrical shells, Journal of Sound and Vibration 255 (2002) 931–963.
[32] F. Moussaoui, R. Benamar, The effects of large vibration amplitudes on the mode shapes and natural frequencies of thin elastics shells. Part III: the non-linear fundamental transverse mode shape, and associated stress distribution for constrained finite circular cylindrical shells. A multi-mode approach, Journal of Sound and Vibration, submitted for publication.
[33] M. El Kadiri, R. Benamar, R.G. White, Improvement of the semi-analytical method, for determining the geometrically non-linear response of thin straight structures. Part I: application to clamped–clamped and simply supported–clamped beams, Journal of Sound and Vibration 249 (2) (2002) 263–305.
[34] M. El Kadiri, R. Benamar, Improvement of the semi-analytical method, for determining the geometrically non-linear response of thin straight structures. Part II: first and second non-linear mode shapes of fully clamped rectangular plates, Journal of Sound and Vibration 257 (2002) 19–62.
[35] M. El Kadiri, R. Benamar, R.G. White, Improvement of the semi-analytical method, for determining the geometrically non-linear response of thin straight structures. Part III: geometrically non-linear steady-state periodic forced response of fully clamped rectangular plates. Applications based on a single mode approach and a simplified multimode approach, Journal of Sound and Vibration, in press.
[36] J.N. Reddy, C.L. Huang, I.R. Singh, Large deflections and large amplitude vibrations of axisymmetric circular plates, International Journal for Numerical Methods in Engineering 17 (1981) 527–541.
[37] S. Timoshenko, S. Woinowsky-Krieger, Theory of Plates and Shells, 2nd Edition, McGraw-Hill, New York, 1959.
[38] W. Han, M. Petyt, Geometrically non-linear vibration analysis of thin, rectangular plates using the hierarchical finite element method-II: first mode of laminated plates and higher modes of isotropic and laminated plates, Computers and Structures 63 (1997) 309–318.
[39] C.Y. Chia, Non-Linear Analysis of Plates, McGraw-Hill, New York, 1980.
[40] A.W. Leissa, Vibrations of Plates, NASA SP-160, U.S. Government Printing Office, Washington, DC, 1969.

[41] M.J.D. Powell, A method for minimising a sum of squares of non-linear functions without calculating derivatives, Computer Journal 7 (1965) 303–307.
[42] M. Sathyamoorthy, Transverse shear and rotatory inertia effects on non-linear vibrations of orthotropic circular plates, Computers and Structures 14 (1981) 129–134.
[43] J. Ramachandran, Frequency analysis of plates vibrating at large amplitudes, Journal of Sound and Vibration 51 (1) (1977) 1–5.
[44] P.C. Dumir, A. Bhaskar, Some erroneous finite element formulations of non-linear vibrations of beams and plates, Journal of Sound and Vibration 123 (3) (1988) 517–527.